MYRISTOYLATED CIL-7 IS REQUIRED FOR POLYCYSTIN ASSOCIATED BEHAVIORS AND EXTRACELLULAR VESICLE BIOGENESIS IN *C. ELEGANS*

By

JULIE ELIZABETH MAGUIRE

A dissertation submitted to the

Graduate School – New Brunswick

and

The Graduate School of Biomedical Sciences

Rutgers, The State University of New Jersey

In partial fulfillment of the requirements

For the degree of

Doctor of Philosophy

Graduate Program in Neuroscience

Written under the direction of

Maureen M. Barr, PhD

And approved by

_____

_____

_____

_____

New Brunswick, New Jersey

May 2015

ABSTRACT OF THE DISSERTATION

Myristoylated CIL-7 is Required for Polycystin Associated Behaviors and Extracellular Vesicle Biogenesis in *C. elegans*

By JULIE ELIZABETH MAGUIRE

Dissertation Director: Dr. Maureen Barr

PKD-2 and LOV-1 are a putative mechanosensory transient receptor potential (TRP) channel-receptor polycystin complex that is required for *C. elegans* male mating behaviors. PKD-2 and LOV-1 localize to cilia found at the end of dendrites of male-specific sensory neurons, which include the CEMs in the head and the RnB neurons and the HOB neuron in the tail. *pkd-2* and *lov-1* mutants are defective in responding to hermaphrodites and locating the hermaphrodite vulva (Barr, DeModena et al. 2001). Mutations in PKD1 and PKD2, the human homologs of *lov-1* and *pkd-2*, cause autosomal dominant polycystic kidney disease (ADPKD). As in *C. elegans*, the mammalian TRP polycystins localize to cilia on renal epithelial cells. The proper placement of PKD-2 to cilia involves several known factors, including LOV-1, intraflagellar transport, and the kinesin-3 KLP-6 (Bae, Qin et al. 2006, Peden, Barr 2005, Hu, Wittekind et al. 2007, Morsci, Barr 2011).

The focus of my research revolved around two mutants, *cil-7(my16)* and *cil-1*(*my15)* that were identified through a forward genetic screen for PKD-2::GFP ciliary localization [Cil] defective mutants (Bae, Lyman-Gingerich et al. 2008,

Bae, Qin et al. 2006). The emphasis of my research work was on the *cil-7(my16)* mutant. Loss of CIL-7 function resulted in a defect in the release of PKD-2::GFP containing extracellular vesicles (EVs) into the external environment, and transmission electron microscopy (TEM) showed that EVs remain trapped in the cephalic lumen. I showed that the myristoylation modification of CIL-7 is required for CIL-7 protein function in PKD-2 localization and *C. elegans* male mating behavior. CIL-7 myristoylation increases CIL-7 association as EV cargo. These studies firmly establish *C. elegans* as an ideal model in which to investigate EV cargo, such as CIL-7, and the acylation modifications that are necessary to become EV-associated.

Acknowledgments

I would first like to thank Dr. Maureen Barr for being a wonderful and awesome advisor during graduate school. She was always never-endingly helpful and kind to me. I thank her so much! I thank my committee members: Dr. Monica Driscoll, Dr. Barth Grant, and Dr. Rongo. The whole Barr lab past and present! A girl cannot get through life without friends so I definitely have to thank my brother from another mother, Dr. Simon Warburton-Pitt who made my graduate days extra special! I would like to thank my graduate school gal pals who are listed in alphabetical order so if they read this they will know I was not playing favorites: Piya Ghose, Cara Nasello, and Suzanne Rzuczek. I also want to thank Tim, Courtney, and Lainey who are my favorite trio! I dedicated this to my parents whom I love so much! They are the best support system a girl could ever ask for!

Table of Contents

Table of Figures

Chapter 1: Introduction

1.1 Cilia and Ciliopathies

1.1.1 Cilia Formation

During the cell cycle at the G1 phase, the mother centriole (which has differentiated into a basal body) nucleates a primary cilium. The cilium resorbs before cell division (Ishikawa, Marshall 2011). Cilia are 5-10μm in length and protrude from the cell thus are known as “cellular antenna” (Fry, Leaper et al. 2014). Vesicles dock at the basal body, fuse, and create what would be the ciliary membrane. After this, the basal body would nucleate the formation of the microtubules, which form the ciliary axoneme (Ishikawa, Marshall 2011, Kim, Dynlacht 2013). The template basal body has nine microtubule triplets and the growing axoneme pushes the ciliary membrane outward (Fry, Leaper et al. 2014). Intraflagellar transport (IFT) helps to form and continually maintain the cilium. IFT was first discovered using *Chlamydomonas reinhardtii* (green alga) (Kozminski, Johnson et al. 1993).

IFT consists of two anterograde kinesin-2 motors (heterotrimeric and homodimeric) and cytoplasmic dynein (Ishikawa, Marshall 2011, Fry, Leaper et al. 2014). The IFT motors transport IFT particles, which are comprised of at least 20 proteins (Mizuno, Taschner et al. 2012, Cole, Diener et al. 1998). The IFT B complex is involved in anterograde transport and the IFT A complex is involved in retrograde transport (Ishikawa, Marshall 2011). IFT also consists of accessory proteins to the IFT B and A complexes and Bardet-Biedl Syndrome (BBS)

proteins (Ishikawa, Marshall 2011).

1.1.2 Cilia Function and Ciliopathies

The primary cilium has the 9+0 axoneme arrangement of nine outer microtubule doublets. The motile cilium has an additional pair of microtubule doublets in the center (9+2). Motile cilia can create a flow and are located for instance in the respiratory tract, oviduct, and ventricular ependymal in the brain (Fry, Leaper et al. 2014). Receptors and channels as well as the components of Hedgehog and Wnt Signaling pathways localize to the ciliary membrane (Satir, Christensen 2007)

Ciliopathies may arise from mutations in ciliary genes. For example, mutations in genes, which encode for instance the BBS proteins, leads to Bardet Biedel Syndrome (Satir, Christensen 2007). Ciliopathies can affect multiple organs (Barker, Thomas et al. 2014). Dysfunctional motile cilia leads to primary ciliary dyskinesia (mucus in airways accumulates) (Fry, Leaper et al. 2014). Nodal cilia have a 9+0 axoneme arrangement and dynein arms, thus move in order to set up left-right patterning. If nodal cilia are dysfunctional, laterality defects occur (Fry, Leaper et al. 2014).

Dysfunctional primary cilia can lead to such diseases as Autosomal Dominant Polycystic Kidney Disease (ADPKD), Bardet Biedl Syndrome (BBS), Joubert Syndrome (JBTS), Meckel-Gruber Syndrome (MKS), Nephronophthisis (NPHP), and retinopathies (Fry, Leaper et al. 2014). ADPKD (the frequency of which is 1:400–1:1,000) arises from mutations in the polycystins *PKD1* and *PKD2,* which leads to kidney cyst formation (Harris, Torres 2014). Studies in model organisms give insight into these ciliopathies. For instance in zebrafish

and mice mutations in ciliary genes create renal cysts (Hildebrandt, Benzing et al. 2011). *C. elegans* is also a useful model in studying cilia. Mutations in *lov-1* and *pkd-2*, which encode polycystins, create males that are defective in several aspects of mating behavior: sex drive, response to hermaphrodite contact and localization of the hermaphrodite vulva (O'Hagan, Wang et al. 2014).

1.2 *C. elegans* Cilia: Ciliated Nervous System, IFT and Ciliary Specialization

1.2.1 Ciliated Nervous System

In the adult hermaphrodite 60 of 302 sensory neurons have a ciliated dendritic ending. These neurons include the amphids, phasmids, inner labial neurons (IL1 and IL2) (Inglis, Ou et al. 2007). The male *C. elegans* has an additional 50 ciliated sensory neurons, which include cephalic male CEM (Male chemotaxis), ray RnA and RnB (Male tail backing and turning), and hook HOA and HOB (Male location of vulva) neurons (Inglis, Ou et al. 2007).

1.2.2 IFT and Ciliary Specialization

The intraflagellar transport (IFT) machinery orchestrates formation and maintenance of cilia and flagella (Ishikawa, Marshall 2011, Fry, Leaper et al. 2014). In *C. elegans* the IFT machinery contains two anterograde motor proteins known as heterotrimeric kinesin-II and homodimeric OSM-3 kinesin-2. Kinesin-II consists of the two motor proteins, KLP-11 and KLP-20 and an accessory protein, KAP-1 (Ishikawa, Marshall 2011). These two motor proteins move the IFT complexes A and B in order to build the cilia. The two complexes collectively have ~20 protein subunits. Complex A works in conjunction with kinesin-II and complex B works in conjunction with OSM-3 (Barr 2005, Peden, Barr 2005,

Silverman, Leroux 2009). The BBS proteins, in particular BBS-7 and BBS-8, have a role in stabilizing the subcomplexes and can act as adaptors for the binding of ciliary proteins to the motor complex (Blacque, Reardon et al. 2004, Silverman, Leroux 2009). The region of the cilium where proteins can enter is the ciliary base/transition zone.

Kinesin-II and OSM-3 kinesin travel together in order to build the middle segments of amphid channel cilia, which are composed of nine microtubule doublets. The OSM-3 kinesin alone constructs the distal segment, which consists of nine microtubule singlets (Snow, Ou et al. 2004, Scholey 2008, O'Hagan, Wang et al. 2014). Kinesin-II and OSM-3 are expressed in all ciliated sensory neurons such as the amphids, phasmids, male-specific neurons, and IL2 neurons (Peden, Barr 2005, Bae, Qin et al. 2006, Ou, Blacque et al. 2005, Evans, Snow et al. 2006). Kinesin-II appears to be a core IFT motor, while OSM-3 may function as an accessory motor (Scholey 2008). For example, the IFT complex B proteins encoded by *che-13*, *osm-1*, and *osm-5* build all cilia however; OSM-3 is not essential in forming IL2 cilia or male-specific CEM cilia (Perkins, Hedgecock et al. 1986, Morsci, Barr 2011).

In amphid channel cilia, kinesin-II moves at a rate of approximately 0.5 µm/sec whereas OSM-3 kinesin moves at a faster rate of approximately 1.3 µm/sec in the anterograde direction. When these two motor proteins are together, their speed is intermediate at approximately 0.7 µm/sec (Snow, Ou et al. 2004). In the process of retrograde movement, the IFT-dynein consists of

CHE-3 which is the dynein heavy chain, XBX-1 which is the light intermediate chain, as well as DYLT-2 which is a light chain (Inglis, Ou et al. 2007).
IFT also has a role in the movement of ciliary membrane proteins such as OSM-9 and OCR-2, which are both transient receptor potential vanilloid (TRPV) channels (Colbert, Smith et al. 1997, Qin, Burnette et al. 2005).

1.3 Polycystins

LOV-1 (PC1 in humans) consists of a large extracellular domain, a GPCR-proteolytic site (GPS), 11 transmembrane domains, and a polycystin-lipoxygenase alpha toxin domain (PLAT). LOV-1 forms a putative mechanosensory receptor-channel complex with PKD-2 (PC2 in humans), a TRP polycystin 2 (TRPP2) channel (Figure 1) (Barr, Sternberg 1999, Bae, Qin et al. 2006, Hu, Wittekind et al. 2007, O'Hagan, Wang et al. 2014). LOV-1 and PKD-2 localize to the cilia and cell bodies of the CEM, RnB, and HOB male-specific sensory neurons (Figure 2). The fully functional PKD-2::GFP is found in neuronal cell bodies and in dendritic and axonal puncta. PKD-2::GFP localizes along the cilium proper, but it is mainly found at the ciliary base (Bae, Qin et al. 2006).

The motor(s) responsible for PKD-2 dendritic transport (or any sensory receptor destined for a cilium in a worm neuron) is unknown (Bae, Qin et al. 2006). The following kinesin and dynein single mutants do not affect PKD-2::GFP distribution: *unc-116(e2310)*/KIF5, *unc-16(ju146, e109)*/JIP3, *klp-10(ok704, tm3750)*/MKLP/CHO1/ZEN-4, *unc-104(e1265)*/KIF1A, *klp-16(ok1505)*/Ncd/KAR3/KLP-3, *dhc-1(or195ts)*[dynein heavy chain homolog], and

dnc-1(or404ts)[a dynactin] (Siddiqui 2002, Bae, Qin et al. 2006). In dendrites the average anterograde velocity of PKD-2::GFP is approximately 1.26 µm/sec and the average retrograde velocity is approximately 0.81 µm/sec. These rates are not statistically different between the CEMs and RnB neurons or for dendritic motility of the ODR-10-GPCR in AWB amphid neurons (Dwyer, Adler et al. 2001). However the average anterograde and retrograde PKD-2::GFP dendritic velocities are statistically different from the rates produced by the IFT machinery (Bae, Qin et al. 2006). Thus, motor proteins distinct from those that make up the IFT machinery drive the transport of ciliary membrane proteins along dendrites.

LOV-1 plays a role in localizing PKD-2 to the cilia. In a *lov-1* mutant PKD-2::GFP aggregates in neuronal cell bodies (Bae, Qin et al. 2006). *unc-101* acts before *lov-1* in the process of somatodendritic sorting (Bae, Qin et al. 2006). *unc-101* also acts before *klp-6* because the Cil phenotype of the *unc-101; klp-6* double mutant resembles the *unc-101* single mutant (Natalia Morsci, Ph.D. thesis). UNC-101 is the µ1 subunit of the AP-1 clathrin adaptor complex, which can bind to a particular transmembrane protein at its cytoplasmic tail. In turn, the adaptor complex is also able to bind to clathrin in order for clathrin to bind to the membrane. Therefore, the adaptor complex provides selectivity of what membrane and cargo form into vesicles (Bonifacino 2014, Dwyer, Adler et al. 2001) (Alberts 2002). In humans, µ1b, is part of the AP-1B clathrin adaptor complex. AP-1B functions in the recycling pathway of the transferrin and LDL receptors (Gravotta, Deora et al. 2007). In *unc-101(m1)* mutants, PKD-2::GFP is visible along the dendrite and the axons as well as the cilium and cell body of

sensory neurons. The increased distribution of PKD-2::GFP along the dendrite in *unc-101(m1)* animals may be the result of the loss of specificity in what cargo is formed. Thus, more than the normal amount of PKD-2::GFP could inadvertently come along for the ride as cargo on vesicles formed by another adaptor complex bound to another transmembrane protein. Therefore, UNC-101 is a key player in PKD-2 targeting to the dendrite. Subsequently, LOV-1 may stabilize PKD-2 within the cell body as well as at its final destination of the cilia (Bae, Qin et al. 2006).

Once at the ciliary base, additional factors come into play in regulating the localization of PKD-2. The PLAT domain of LOV-1 binds to the β subunit of the casein kinase II (CK2) (Hu, Barr 2005, Hu, Bae et al. 2006). CK2 potentially phosphorylates PKD-2 on serine 534 with the phosphatase calcineurin dephosphorylating PKD-2. Hu et al. (2006) propose that LOV-1 binds to CK2, and when stimulated mechanically, PKD-2 becomes phosphorylated by CK2 allowing more calcium to enter, and, in turn, triggering calcineurin to dephosphorylate and inactivate PKD-2. The STAM-Hrs complex removes constitutively active PKD-2 from the ciliary membrane (Hu, Bae et al. 2006).

STAM (signal transducing adaptor molecule) and Hrs (hepatocyte growth factor regulated tyrosine kinase substrate) sequester the mechanosensory receptor-channel complex for lysosomal degradation. STAM binds to the C-terminus of LOV-1. The proposed model for downregulation of the receptor-channel complex involves the STAM-Hrs complex contacting ubiquitinated PKD-

2 in the process of directing the receptor-channel complex from the early endosome to the lysosome for degradation (Hu, Wittekind et al. 2007).

The kinesin-3, KLP-6, is necessary for the proper localization of PKD-2::GFP. KLP-6::GFP is coexpressed with *lov-1* and *pkd-2* in adult male-specific sensory neurons and is also expressed in the IL2 neurons, which are found in both the male and hermaphrodite nervous system. Similar to *lov-1* and *pkd-2* mutants, *klp-6* males are response and Lov defective (Peden, Barr 2005). In *klp-6* mutant males, PKD-2::GFP forms bright puncta at the ciliary bases of the CEM neurons and increased localization along the dendrites of the RnB and HOB neurons. PKD-2::GFP is decreased in the ray cilia of *klp-6* males. In *klp-6* animals, PKD-2::GFP dendritic motility is not affected (Peden, Barr 2005, Bae, Qin et al. 2006) (Dr. Natalia Morsci, Ph.D. thesis). Thus, KLP-6 is proposed to transport PKD-2 along cilia or act as a tether between the polycystins and the microtubules (Peden, Barr 2005, Bae, Qin et al. 2006).

A forward genetic screen identified additional regulators of PKD-2 localization (Bae, Lyman-Gingerich et al. 2008). The ciliary localization (Cil) defective mutants were separated into either Class A, which is characterized by a distinguishable PKD-2::GFP accumulation in the dendrites of CEMs (an *unc-101* like phenotype), or into Class B, which is characterized by a distinguishable PKD-2::GFP accumulation at the cilia or cilia bases (a *klp-6* like phenotype) (Bae, Lyman-Gingerich et al. 2008). My thesis work focuses on *cil-7(my16)* and *cil-1(my15)*, two mutants isolated in the screen.

While *cil-7* and *cil-1* mutants both affect PKD-2::GFP distribution, each is

unique in the set of phenotypes each produces. *cil-1* is a class A mutant while *cil-7* is a class B. *cil-1* encodes a phosphoinositide 5-phosphatase (Bae, Kim et al. 2009). The gene mutated in *cil-7(my16)* animals was not known. Thus, the major goals of my project were two-fold. First, I cloned and characterized the *cil-7* gene and determined the mechanism by which CIL-7 regulated PKD-2 ciliary localization (Chapters 2 and 3). Second, I resolved unanswered questions regarding CIL-1 and the role of phosphoinositides in ciliary receptor localization (Chapter 4).

1.4 Myristoylation and Extracellular Vesicles of Flagella and Cilia

1.4.1 Myristoylation

The interest in myristoylation lies in the fact that the main protein that I focused on for my graduate work was CIL-7, a putatively myristoylated protein. CIL-7 is targeted to extracellular vesicles (EVs) as cargo by its myristoylation motif and is subsequently released outside of the exposed cilium. CIL-7 as a membrane bound protein has a role in the localization and release of polycystin-containing EVs. Thus, I was interested to learn how acyl modifications such as myristoylation could target a protein to flagella and cilia and additionally how acyl modifications could target proteins to EVs.

The addition of the myristoyl group usually occurs co-translationally. In order for the protein to bind more stably to the membrane, the myristoyl group is accompanied either by a palmitoyl addition or a polybasic region (Resh 2013). The fatty acylation by myristoylation and/or palmitoylation targets proteins to cilia

or flagella. In *Leishmania major,* the small myristoylated protein-1(SMP-1) is targeted to the flagella by myristoylation and palmitoylation (Tull, Naderer et al. 2010, Tull, Vince et al. 2004). Similarly, the *Trpanosoma cruzi* protein, flagellar calcium-binding protein (FCaBP), localizes to the flagella by being myristoylated and palmitoylated (Godsel, Engman 1999, Maric, McGwire et al. 2011, Maric, Epting et al. 2010). *C.elegans* serine/threonine protein phosphatase of the RdgC/PPEF family (CePPEF) is dependent on myristoylation and palmitoylation for its localization to the cilia of the AWB and AWC sensory neurons (Ramulu, Nathans 2001). In *C. elegans*, ADP-ribosylation factor-like protein 13B (Arl13b) utilizes palmitoylation in order to associate with the ciliary membrane (Cevik, Hori et al. 2010).

Myristoylation targets mammalian nephrocystin-3 (NPHP3) to the ciliary shaft (Nakata, Shiba et al. 2012). The mammalian cystin protein when mutated in mice provides a model for human autosomal recessive PKD (ARPKD) (Hou, Mrug et al. 2002). In the mammalian system PC1, PC2, and cystin do colocalize in cilia (Yoder, Hou et al. 2002). Cystin is myristoylated and fractionates with lipid raft fractions (Tao, Bu et al. 2009, Hurd, Margolis 2009). Myristoylation and palmitoylation target mammalian retinitis pigmentosa protein (RP2) to the ciliary base (Chapple, Hardcastle et al. 2000). RP2 functions as a GTPase activating protein (GAP) for ARL3 (Veltel, Gasper et al. 2008, Evans, Schwarz et al. 2010). Mammalian UNC-119b binds NPHP3 and cystin through their myristoylation modification and traffics them to the cilium (Wright, Baye et al. 2011). UNC119 releases its cargo into the ciliary membrane through the action of ARL3, and RP2

subsequently activates ARL3 in order to release it from UNC-119b (Wright, Baye et al. 2011).

1.4.2 Extracellular Vesicles of Flagella and Cilia

EVs act in intercellular communication in such examples as the transfer of mRNA and miRNA, coagulation, inflammation, and the talk between neurons and glia in the nervous system. EVs can form as plasma membrane budding off to create microvesicles/ectosomes (100-1,000 nm). EVs can also form from the multivesicular body (MVB)/ late endosome fusing with the plasma membrane and releasing its contents (40-100 nm) (Cocucci, Racchetti et al. 2009, Raposo, Stoorvogel 2013). Cilia and flagella provide information out into the environment through the release of vesicles (Avasthi, Marshall 2013). In *Chlamydomonas*, ciliary ectosomes released from the flagella contain PKD-2 as well as the vegetative lytic enzyme (VLE) (Wood, Huang et al. 2013).

In *C. elegans*, the male-specific B type sensory neurons as well as the shared IL2 neurons all have an exposed cilium where EVs are released into the environment after being shed from the cilium (Wang, Silva et al. 2014). We refer to the collection of the male-specific B type sensory neurons and the shared IL2 neurons as the 27 EV-Releasing Neurons. LOV-1::GFP and PKD-2::GFP are shed and released, unlike cilium structural components (GFP-tagged b-tubulin TBB-4), IFT polypeptides (IFT-B polypeptide IFT52/OSM-6), or ciliary motors (kinesin-II and KLP-6) (Wang, Silva et al. 2014). The male-specific B type sensory neurons and the shared IL2 neurons shed and release the protein

coexpressed with polycystin-1 (CWP-1). The release of PKD-2::GFP requires the IFT machinery and KLP-6 (Wang, Silva et al. 2014).

EVs produced by *C. elegans* males induce a male tail-chasing behavior. Thus, EVs can also provide a form of animal communication (Wang, Silva et al. 2014).

Myristoylated proteins such as *Trpanosoma cruzi* flagellar calcium-binding protein (FCaBP) and mammalian Retinitis pigmentosa-2 (RP2) are vesicle cargo (Ouaissi, Aguirre et al. 1992, Emmer, Maric et al. 2010). RP2 interacts and forms a complex with PC2 that requires RP2 being acylated. RP2 and PC2 are also secreted by Madin-Darby Canine Kidney Epithelial Cells (MDCK) from the apical side, and RP2 is needed in order for PC2 to be secreted (Hurd, Zhou et al. 2010). PC1 was detected to associate with vesicles (exosomes) obtained from human urine (Pisitkun, Shen et al. 2004). Hogan et al., went on to show that exosome-like vesicles (ELVs) from human urine are not only associated with PC1 but also PC2, fibrocystin (FCP), ARL6, and cystin. ELVs associate along primary cilia of kidney and biliary epithelial cells (Hogan, Manganelli et al. 2009).

Acylation can also target proteins as cargo for vesicle secretion. How a known cytoplasmic protein can be instead targeted for secretion was addressed using the yeast protein TyA in Jurkat T cells (Fang, Wu et al. 2007). TyA-GFP with an acylation tag that includes a myristoylation site and a palmitoylation site directed this protein to endosome-like domains (ELDs) of the plasma membrane, whereas a tag mutated for the acylation sites did not (Fang, Wu et al. 2007).

Thus, fatty acylation can potentially help to target proteins to cilia and flagella, and these modifications may also associate proteins with EVs as cargo.

The use of *C. elegans* and the characterization of CIL-7 provided insight into EV biogenesis and targeting mechanisms and demonstrated that protein modifications such as myristoylation act in targeting cargo to EVs and in protein function. Thus, CIL-7 is an EV regulator like the IFT machinery and KLP-6.

1.5 Figures for Chapter 1

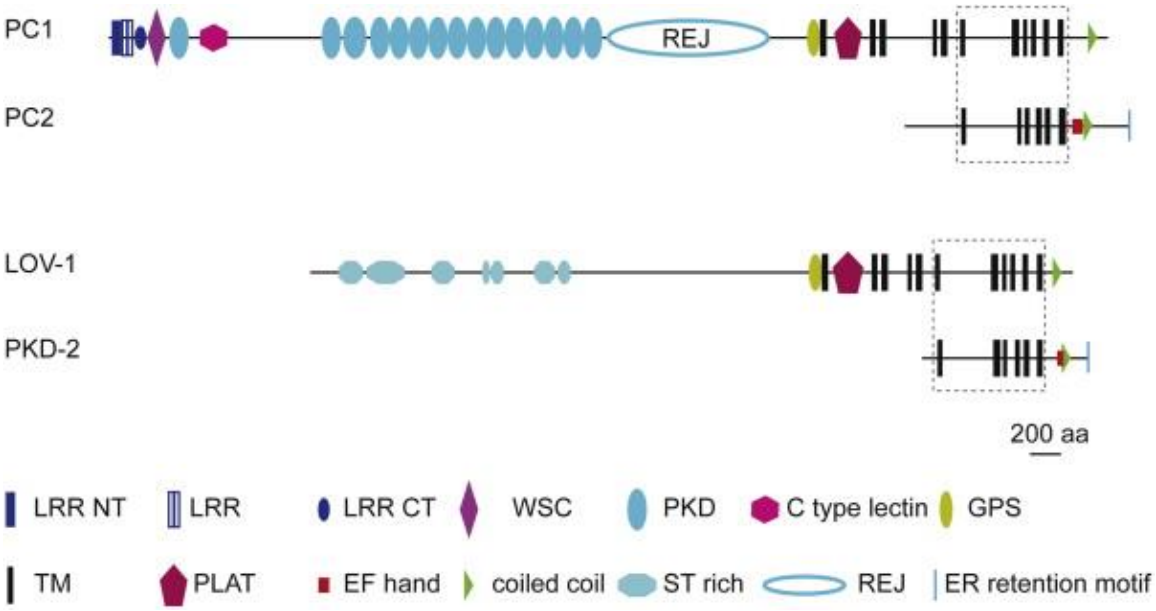

Figure 1. Reproduced from O'Hagan, Wang et al. 2014 the Schematic Depicts Functional Domains for Human PC1 and PC2 and *C. elegans* LOV-1 and PKD-2

The reproduced figure from O'Hagan, Wang et al. 2014 depicts the functional domains of Human PC1 and PC2 and *C. elegans* LOV-1 and PKD-2. (Abbreviations: LRR, leucine-rich repeat; WSC, cell wall integrity and stress response component; PKD, polycystic kidney disease domain; GPS, GPCR proteolytic site; TM, transmembrane; PLAT, polycystin/lipoxygenase/ α -toxin; ST rich, serine-threonine rich.)

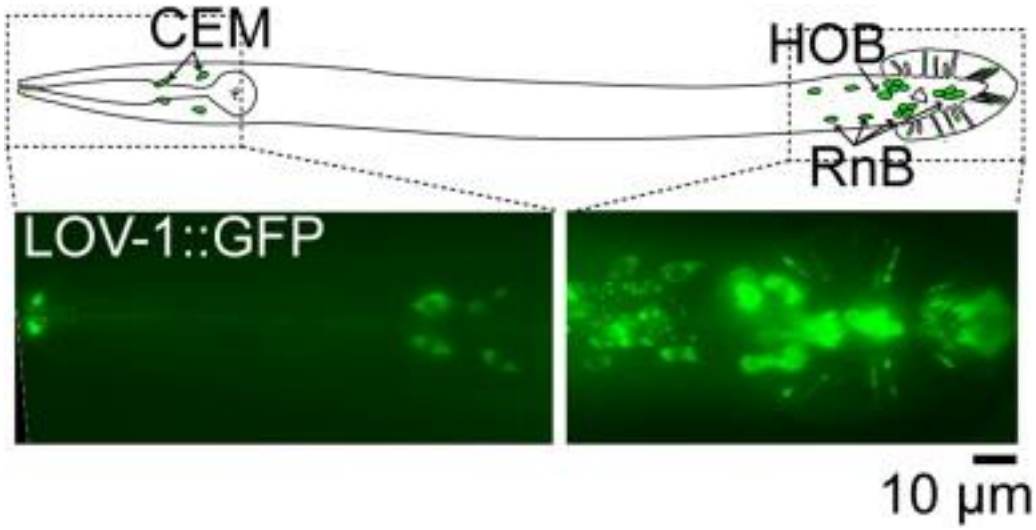
CEM
HOB
RnB
LOV-1::GFP
10 µm

Figure 2. Reproduced from O'Hagan, Wang et al. 2014 Depicts the Expression of the LOV-1::GFP Reporter. Like PKD-2::GFP, LOV-1::GFP is Expressed in the Cell Bodies and the Sensory Cilia of the CEM, RnB, and HOB Male Neurons

The reproduced figure from O'Hagan, Wang et al. 2014 highlights the male sensory neurons and where they reside in the male *C. elegans* animal. This figure also highlights LOV-1 expression in these neurons, which are the cell bodies and the sensory cilia.

1.6 References

AVASTHI, P. and MARSHALL, W., 2013. Ciliary secretion: switching the cellular antenna to 'transmit'. *Current biology : CB,* **23**(11), pp. R471-3.

BAE, Y.K., KIM, E., L'HERNAULT, S.W. and BARR, M.M., 2009. The CIL-1 PI 5-phosphatase localizes TRP Polycystins to cilia and activates sperm in C. elegans. *Current biology : CB,* **19**(19), pp. 1599-1607.

BAE, Y.K., LYMAN-GINGERICH, J., BARR, M.M. and KNOBEL, K.M., 2008. Identification of genes involved in the ciliary trafficking of C. elegans PKD-2. *Developmental dynamics : an official publication of the American Association of Anatomists,* **237**(8), pp. 2021-2029.

BAE, Y.K., QIN, H., KNOBEL, K.M., HU, J., ROSENBAUM, J.L. and BARR, M.M., 2006. General and cell-type specific mechanisms target TRPP2/PKD-2 to cilia. *Development (Cambridge, England),* **133**(19), pp. 3859-3870.

BARKER, A.R., THOMAS, R. and DAWE, H.R., 2014. Meckel-Gruber syndrome and the role of primary cilia in kidney, skeleton, and central nervous system development. *Organogenesis,* **10**(1), pp. 96-107.

BARR, M.M., 2005. Caenorhabditis elegans as a model to study renal development and disease: sexy cilia. *Journal of the American Society of Nephrology : JASN,* **16**(2), pp. 305-312.

BARR, M.M. and STERNBERG, P.W., 1999. A polycystic kidney-disease gene homologue required for male mating behaviour in C. elegans. *Nature,* **401**(6751), pp. 386-389.

BLACQUE, O.E., REARDON, M.J., LI, C., MCCARTHY, J., MAHJOUB, M.R., ANSLEY, S.J., BADANO, J.L., MAH, A.K., BEALES, P.L., DAVIDSON, W.S., JOHNSEN, R.C., AUDEH, M., PLASTERK, R.H., BAILLIE, D.L., KATSANIS, N., QUARMBY, L.M., WICKS, S.R. and LEROUX, M.R., 2004. Loss of C. elegans BBS-7 and BBS-8 protein function results in cilia defects and compromised intraflagellar transport. *Genes & development,* **18**(13), pp. 1630-1642.

BONIFACINO, J.S., 2014. Adaptor proteins involved in polarized sorting. *The Journal of cell biology,* **204**(1), pp. 7-17.

CEVIK, S., HORI, Y., KAPLAN, O.I., KIDA, K., TOIVENON, T., FOLEY-FISHER, C., COTTELL, D., KATADA, T., KONTANI, K. and BLACQUE, O.E., 2010. Joubert syndrome Arl13b functions at ciliary membranes and stabilizes protein transport in Caenorhabditis elegans. *The Journal of cell biology,* **188**(6), pp. 953-969.

CHAPPLE, J.P., HARDCASTLE, A.J., GRAYSON, C., SPACKMAN, L.A., WILLISON, K.R. and CHEETHAM, M.E., 2000. Mutations in the N-terminus of the X-linked retinitis pigmentosa protein RP2 interfere with the normal targeting of the protein to the plasma membrane. *Human molecular genetics,* **9**(13), pp. 1919-1926.

COCUCCI, E., RACCHETTI, G. and MELDOLESI, J., 2009. Shedding microvesicles: artefacts no more. *Trends in cell biology,* **19**(2), pp. 43-51.

COLBERT, H.A., SMITH, T.L. and BARGMANN, C.I., 1997. OSM-9, a novel protein with structural similarity to channels, is required for olfaction, mechanosensation, and olfactory adaptation in Caenorhabditis elegans. *The Journal of neuroscience : the official journal of the Society for Neuroscience,* **17**(21), pp. 8259-8269.

COLE, D.G., DIENER, D.R., HIMELBLAU, A.L., BEECH, P.L., FUSTER, J.C. and ROSENBAUM, J.L., 1998. Chlamydomonas kinesin-II-dependent intraflagellar transport (IFT): IFT particles contain proteins required for ciliary assembly in Caenorhabditis elegans sensory neurons. *The Journal of cell biology,* **141**(4), pp. 993-1008.

DWYER, N.D., ADLER, C.E., CRUMP, J.G., L'ETOILE, N.D. and BARGMANN, C.I., 2001. Polarized dendritic transport and the AP-1 mu1 clathrin adaptor UNC-101 localize odorant receptors to olfactory cilia. *Neuron,* **31**(2), pp. 277-287.

EMMER, B.T., MARIC, D. and ENGMAN, D.M., 2010. Molecular mechanisms of protein and lipid targeting to ciliary membranes. *Journal of cell science,* **123**(Pt 4), pp. 529-536.

EVANS, J.E., SNOW, J.J., GUNNARSON, A.L., OU, G., STAHLBERG, H., MCDONALD, K.L. and SCHOLEY, J.M., 2006. Functional modulation of IFT kinesins extends the sensory repertoire of ciliated neurons in Caenorhabditis elegans. *The Journal of cell biology,* **172**(5), pp. 663-669.

EVANS, R.J., SCHWARZ, N., NAGEL-WOLFRUM, K., WOLFRUM, U., HARDCASTLE, A.J. and CHEETHAM, M.E., 2010. The retinitis pigmentosa protein RP2 links pericentriolar vesicle transport between the Golgi and the primary cilium. *Human molecular genetics,* **19**(7), pp. 1358-1367.

FANG, Y., WU, N., GAN, X., YAN, W., MORRELL, J.C. and GOULD, S.J., 2007. Higher-order oligomerization targets plasma membrane proteins and HIV gag to exosomes. *PLoS biology,* **5**(6), pp. e158.

FRY, A.M., LEAPER, M.J. and BAYLISS, R., 2014. The primary cilium: guardian of organ development and homeostasis. *Organogenesis,* **10**(1), pp. 62-68.

GODSEL, L.M. and ENGMAN, D.M., 1999. Flagellar protein localization mediated by a calcium-myristoyl/palmitoyl switch mechanism. *The EMBO journal,* **18**(8), pp. 2057-2065.

GRAVOTTA, D., DEORA, A., PERRET, E., OYANADEL, C., SOZA, A., SCHREINER, R., GONZALEZ, A. and RODRIGUEZ-BOULAN, E., 2007. AP1B sorts basolateral proteins in recycling and biosynthetic routes of MDCK cells. *Proceedings of the National Academy of Sciences of the United States of America,* **104**(5), pp. 1564-1569.

HARRIS, P.C. and TORRES, V.E., 2014. Genetic mechanisms and signaling pathways in autosomal dominant polycystic kidney disease. *The Journal of clinical investigation,* **124**(6), pp. 2315-2324.

HILDEBRANDT, F., BENZING, T. and KATSANIS, N., 2011. Ciliopathies. *The New England journal of medicine,* **364**(16), pp. 1533-1543.

HOGAN, M.C., MANGANELLI, L., WOOLLARD, J.R., MASYUK, A.I., MASYUK, T.V., TAMMACHOTE, R., HUANG, B.Q., LEONTOVICH, A.A., BEITO, T.G., MADDEN, B.J., CHARLESWORTH, M.C., TORRES, V.E., LARUSSO, N.F., HARRIS, P.C. and WARD, C.J., 2009. Characterization of PKD protein-positive exosome-like vesicles. *Journal of the American Society of Nephrology : JASN,* **20**(2), pp. 278-288.

HOU, X., MRUG, M., YODER, B.K., LEFKOWITZ, E.J., KREMMIDIOTIS, G., D'EUSTACHIO, P., BEIER, D.R. and GUAY-WOODFORD, L.M., 2002. Cystin, a novel cilia-associated protein, is disrupted in the cpk mouse model of polycystic kidney disease. *The Journal of clinical investigation,* **109**(4), pp. 533-540.

HU, J., BAE, Y.K., KNOBEL, K.M. and BARR, M.M., 2006. Casein kinase II and calcineurin modulate TRPP function and ciliary localization. *Molecular biology of the cell,* **17**(5), pp. 2200-2211.

HU, J. and BARR, M.M., 2005. ATP-2 interacts with the PLAT domain of LOV-1 and is involved in Caenorhabditis elegans polycystin signaling. *Molecular biology of the cell,* **16**(2), pp. 458-469.

HU, J., WITTEKIND, S.G. and BARR, M.M., 2007. STAM and Hrs down-regulate ciliary TRP receptors. *Molecular biology of the cell,* **18**(9), pp. 3277-3289.

HURD, T., ZHOU, W., JENKINS, P., LIU, C.J., SWAROOP, A., KHANNA, H., MARTENS, J., HILDEBRANDT, F. and MARGOLIS, B., 2010. The retinitis pigmentosa protein RP2 interacts with polycystin 2 and regulates cilia-mediated vertebrate development. *Human molecular genetics,* **19**(22), pp. 4330-4344.

HURD, T.W. and MARGOLIS, B., 2009. Cystin, cilia, and cysts: unraveling trafficking determinants. *Journal of the American Society of Nephrology : JASN,* **20**(12), pp. 2485-2486.

INGLIS, P.N., OU, G., LEROUX, M.R. and SCHOLEY, J.M., 2007. The sensory cilia of Caenorhabditis elegans. *WormBook : the online review of C.elegans biology,* , pp. 1-22.

ISHIKAWA, H. and MARSHALL, W.F., 2011. Ciliogenesis: building the cell's antenna. *Nature reviews.Molecular cell biology,* **12**(4), pp. 222-234.

KIM, S. and DYNLACHT, B.D., 2013. Assembling a primary cilium. *Current opinion in cell biology,* **25**(4), pp. 506-511.

KOZMINSKI, K.G., JOHNSON, K.A., FORSCHER, P. and ROSENBAUM, J.L., 1993. A motility in the eukaryotic flagellum unrelated to flagellar beating. *Proceedings of the National Academy of Sciences of the United States of America,* **90**(12), pp. 5519-5523.

MARIC, D., EPTING, C.L. and ENGMAN, D.M., 2010. Composition and sensory function of the trypanosome flagellar membrane. *Current opinion in microbiology,* **13**(4), pp. 466-472.

MARIC, D., MCGWIRE, B.S., BUCHANAN, K.T., OLSON, C.L., EMMER, B.T., EPTING, C.L. and ENGMAN, D.M., 2011. Molecular determinants of ciliary membrane localization of Trypanosoma cruzi flagellar calcium-binding protein. *The Journal of biological chemistry,* **286**(38), pp. 33109-33117.

MIZUNO, N., TASCHNER, M., ENGEL, B.D. and LORENTZEN, E., 2012. Structural studies of ciliary components. *Journal of Molecular Biology,* **422**(2), pp. 163-180.

MORSCI, N.S. and BARR, M.M., 2011. Kinesin-3 KLP-6 regulates intraflagellar transport in male-specific cilia of Caenorhabditis elegans. *Current biology : CB,* **21**(14), pp. 1239-1244.

NAKATA, K., SHIBA, D., KOBAYASHI, D. and YOKOYAMA, T., 2012. Targeting of Nphp3 to the primary cilia is controlled by an N-terminal myristoylation site and coiled-coil domains. *Cytoskeleton (Hoboken, N.J.),* **69**(4), pp. 221-234.

O'HAGAN, R., WANG, J. and BARR, M.M., 2014. Mating behavior, male sensory cilia, and polycystins in Caenorhabditis elegans. *Seminars in cell & developmental biology,* **33**, pp. 25-33.

OU, G., BLACQUE, O.E., SNOW, J.J., LEROUX, M.R. and SCHOLEY, J.M., 2005. Functional coordination of intraflagellar transport motors. *Nature,* **436**(7050), pp. 583-587.

OUAISSI, A., AGUIRRE, T., PLUMAS-MARTY, B., PIRAS, M., SCHONECK, R., GRAS-MASSE, H., TAIBI, A., LOYENS, M., TARTAR, A. and CAPRON, A., 1992. Cloning and sequencing of a 24-kDa Trypanosoma cruzi specific antigen released in association with membrane vesicles and defined by a monoclonal antibody. *Biology of the cell / under the auspices of the European Cell Biology Organization,* **75**(1), pp. 11-17.

PEDEN, E.M. and BARR, M.M., 2005. The KLP-6 kinesin is required for male mating behaviors and polycystin localization in Caenorhabditis elegans. *Current biology : CB,* **15**(5), pp. 394-404.

PERKINS, L.A., HEDGECOCK, E.M., THOMSON, J.N. and CULOTTI, J.G., 1986. Mutant sensory cilia in the nematode Caenorhabditis elegans. *Developmental biology,* **117**(2), pp. 456-487.

PISITKUN, T., SHEN, R.F. and KNEPPER, M.A., 2004. Identification and proteomic profiling of exosomes in human urine. *Proceedings of the National Academy of Sciences of the United States of America,* **101**(36), pp. 13368-13373.

QIN, H., BURNETTE, D.T., BAE, Y.K., FORSCHER, P., BARR, M.M. and ROSENBAUM, J.L., 2005. Intraflagellar transport is required for the vectorial movement of TRPV channels in the ciliary membrane. *Current biology : CB,* **15**(18), pp. 1695-1699.

RAMULU, P. and NATHANS, J., 2001. Cellular and subcellular localization, N-terminal acylation, and calcium binding of Caenorhabditis elegans protein phosphatase with EF-hands. *The Journal of biological chemistry,* **276**(27), pp. 25127-25135.

RAPOSO, G. and STOORVOGEL, W., 2013. Extracellular vesicles: exosomes, microvesicles, and friends. *The Journal of cell biology,* **200**(4), pp. 373-383.

RESH, M.D., 2013. Covalent lipid modifications of proteins. *Current biology : CB,* **23**(10), pp. R431-5.

SATIR, P. and CHRISTENSEN, S.T., 2007. Overview of structure and function of mammalian cilia. *Annual Review of Physiology,* **69**, pp. 377-400.

SCHOLEY, J.M., 2008. Intraflagellar transport motors in cilia: moving along the cell's antenna. *The Journal of cell biology,* **180**(1), pp. 23-29.

SIDDIQUI, S.S., 2002. Metazoan motor models: kinesin superfamily in C. elegans. *Traffic (Copenhagen, Denmark),* **3**(1), pp. 20-28.

SILVERMAN, M.A. and LEROUX, M.R., 2009. Intraflagellar transport and the generation of dynamic, structurally and functionally diverse cilia. *Trends in cell biology,* **19**(7), pp. 306-316.

SNOW, J.J., OU, G., GUNNARSON, A.L., WALKER, M.R., ZHOU, H.M., BRUST-MASCHER, I. and SCHOLEY, J.M., 2004. Two anterograde intraflagellar transport motors cooperate to build sensory cilia on C. elegans neurons. *Nature cell biology,* **6**(11), pp. 1109-1113.

TAO, B., BU, S., YANG, Z., SIROKY, B., KAPPES, J.C., KISPERT, A. and GUAY-WOODFORD, L.M., 2009. Cystin localizes to primary cilia via membrane microdomains and a targeting motif. *Journal of the American Society of Nephrology : JASN,* **20**(12), pp. 2570-2580.

TULL, D., NADERER, T., SPURCK, T., MERTENS, H.D., HENG, J., MCFADDEN, G.I., GOOLEY, P.R. and MCCONVILLE, M.J., 2010. Membrane protein SMP-1 is required for normal flagellum function in Leishmania. *Journal of cell science,* **123**(Pt 4), pp. 544-554.

TULL, D., VINCE, J.E., CALLAGHAN, J.M., NADERER, T., SPURCK, T., MCFADDEN, G.I., CURRIE, G., FERGUSON, K., BACIC, A. and MCCONVILLE, M.J., 2004. SMP-1, a member of a new family of small myristoylated proteins in kinetoplastid parasites, is targeted to the flagellum membrane in Leishmania. *Molecular biology of the cell,* **15**(11), pp. 4775-4786.

VELTEL, S., GASPER, R., EISENACHER, E. and WITTINGHOFER, A., 2008. The retinitis pigmentosa 2 gene product is a GTPase-activating protein for Arf-like 3. *Nature structural & molecular biology,* **15**(4), pp. 373-380.

WANG, J., SILVA, M., HAAS, L.A., MORSCI, N.S., NGUYEN, K.C., HALL, D.H. and BARR, M.M., 2014. C. elegans Ciliated Sensory Neurons Release Extracellular Vesicles that Function in Animal Communication. *Current biology : CB,* **24**(5), pp. 519-525.

WOOD, C.R., HUANG, K., DIENER, D.R. and ROSENBAUM, J.L., 2013. The cilium secretes bioactive ectosomes. *Current biology : CB,* **23**(10), pp. 906-911.

WRIGHT, K.J., BAYE, L.M., OLIVIER-MASON, A., MUKHOPADHYAY, S., SANG, L., KWONG, M., WANG, W., PRETORIUS, P.R., SHEFFIELD, V.C., SENGUPTA, P., SLUSARSKI, D.C. and JACKSON, P.K., 2011. An ARL3-UNC119-RP2 GTPase cycle targets myristoylated NPHP3 to the primary cilium. *Genes & development,* **25**(22), pp. 2347-2360.

YODER, B.K., HOU, X. and GUAY-WOODFORD, L.M., 2002. The polycystic kidney disease proteins, polycystin-1, polycystin-2, polaris, and cystin, are co-localized in renal cilia. *Journal of the American Society of Nephrology : JASN,* **13**(10), pp. 2508-2516.

Chapter 2: Myristoylation is Essential for Ciliary EV Cargo Association and Function

Note: This chapter is partially reproduced from sections of the following: Maguire, J. E., Silva, M., Nguyen, K.C., Hellen, E., Kern A., Hall, D.H., and Barr, M. M. (2015). Myristoylation is Essential for Ciliary EV Cargo Association and Function. (Submitted to MBoC)

2.1 Abstract

The cilium both releases and binds to extracellular vesicles (EVs) (Wood, Huang et al. 2013, Hogan, Manganelli et al. 2009, Wang, Silva et al. 2014, Pampliega, Orhon et al. 2013). EVs may be used by cells as a form of intercellular communication and mediate a broad range of physiological and pathological processes (Gyorgy, Szabo et al. 2011). The mammalian polycystins (PCs) localize to cilia as well as urinary EVs released from renal epithelial cells (Hogan, Manganelli et al. 2009). PC ciliary trafficking defects may be an underlying cause of autosomal dominant polycystic kidney disease (Cai, Fedeles et al. 2014), and ciliary-EV interactions have been proposed to play a central role in the biology of PKD (Chacon-Heszele, Choi et al. 2014). In *C. elegans* and mammals, PC1 and PC2 act in the same genetic pathway, act in a sensory capacity, localize to cilia, and are contained in secreted EVs, suggesting ancient conservation (Hogan, Manganelli et al. 2009, Wang, Silva et al. 2014, O'Hagan, Wang et al. 2014). However, the relationship between cilia and EVs and the mechanisms generating PC-containing EVs remain an enigma. In a forward

genetic screen for regulators of *C. elegans* PKD-2 ciliary localization (Bae, Lyman-Gingerich et al. 2008), we identified CIL-7, a myristoylated protein that regulates EV biogenesis. Loss of CIL-7 results in male mating behavioral defects, excessive accumulation of EVs in the lumen of the cephalic sensory organ, and failure to release PKD-2::GFP-containing EVs to the environment. Fatty acylation, such as myristoylation and palmitoylation, targets proteins to cilia and flagella (Tull, Naderer et al. 2010, Godsel, Engman 1999, Maric, McGwire et al. 2011, Ramulu, Nathans 2001, Cevik, Sanders et al. 2013, Wright, Baye et al. 2011, Tao, Bu et al. 2009). The CIL-7 myristoylation motif is essential for CIL-7 function and for targeting CIL-7 to EVs. *C. elegans* is a powerful model to study ciliary EV biogenesis in vivo and to identify cis-targeting motifs such as myristoylation that are necessary for EV-cargo association and function.

2.2 Results

2.3.1 Myristoylated CIL-7 is Required for Polycystin Localization

The *C. elegans* PCs LOV-1 and PKD-2 localize to the cilia of 21 male-specific ciliated sensory neurons (Figure 3A, G), which are the cephalic male neurons (CEM), hook B type (HOB) neuron, and the ray B type (RnB, where n=1-9, excluding 6) neurons (Barr, DeModena et al. 2001, Barr, Sternberg 1999). *lov-1* and *pkd-2* are required for several male-specific mating behaviors, including sex drive, response to hermaphrodite contact, and location of the hermaphrodite's vulva (Barr, Sternberg 1999, Barr, DeModena et al. 2001, Barrios, Nurrish et al. 2008). *C. elegans* is a powerful system for identifying genes that are important

for PC localization and function (O'Hagan, Wang et al. 2014). One such regulator of PKD-2 localization is the kinesin-like protein 6 (KLP-6) of the kinesin-3 family (Peden, Barr 2005). *klp-6* regulates intraflagellar transport (IFT), EV release, and PKD-2::GFP targeting to EVs (Morsci, Barr 2011). *klp-6* mutant males accumulate PKD-2::GFP at ciliary bases and are response (Rsp) and location of vulva (Lov) defective (Peden, Barr 2005). *klp-6* is coexpressed with the polycystins in the 21 male-specific B type ciliated sensory neurons and also in six shared IL2 neurons (found in both males and hermaphrodites). Each of these 27 *klp-6* expressing sensory neurons has an environmentally exposed cilium that penetrates the cuticle and possesses the unique ability to shed and release EVs to the environment. Herein we refer to these as the EV-releasing ciliated sensory neurons.

The *cil-7(my16)* mutant was isolated in a forward genetic screen for regulators of PKD-2::GFP ciliary localization (Bae, Lyman-Gingerich et al. 2008). *my16* males accumulated PKD-2::GFP at ciliary bases and displayed a Cil (ciliary localization) phenotype (Figure 3B). We used a combination of single nucleotide polymorphism (SNP) mapping, deficiency mapping and whole genome sequencing (WGS) and determined that *my16* was a mutation in the open reading frame of W03G9.7. A fosmid or a single gene construct of W03G9.7 rescued the *my16* Cil phenotype (Figure 4A). Two other alleles, *gk688330* and *tm5848*, phenocopy the Cil phenotype of *my16* (Figure 3C and D), fail to complement *my16* (Figure 4B), and so affect W03G9.7 (E). We conclude that *my16* is a missense mutation in W03G9.7, which we refer to as *cil-7*.

cil-7 encodes a predicted protein with a myristoylation motif followed by five coiled-coil domains and a leucine zipper (Figure 3F). CIL-7 contains a 17 amino acid sequence predicted to be recognized by N-myristoyltransferase (NMT), which co-translationally adds a 14-carbon saturated fatty acid to the N-terminal glycine (Eisenhaber, Eisenhaber et al. 2003). The myristoyl group is usually accompanied by a polybasic region or a palmitoyl addition to enable stable membrane association (Resh 2013). Homology searches using the complete NCBI nr database reveal that CIL-7 has homologs in many invertebrate genomes but not in vertebrate lineages (Figure 4C). Further, the 17 aa myristoylation sequence is completely conserved in *Caenorhabditis* species, and the CIL-7 Gly2 is conserved in most species identified. The 3rd amino acid (CIL-7 Ser3) is a Cys in more highly diverged species (Figure 4D).

The *my16* and *gk688330* alleles disrupt the CIL-7 myristoylation motif (Figure 3E, F). Proteins that are covalently myristoylated generally contain the sequence Met-Gly-X-X-X-Ser/Thr at the amino terminus. In the NMT recognition sequence, the glycine residue is where the myristoyl moiety is added. In the *cil-7(gk688330)* mutant, this Gly is changed to Asp. The binding pocket of NMT is narrow, requiring the residue following Gly to be small, such as Ser in CIL-7 (Maurer-Stroh, Eisenhaber et al. 2002). If this residue is Phe, Lys, Tyr, Trp, or Arg, myristoylation is inhibited (Utsumi, Sato et al. 2001). In the *cil-7(my16)* mutant, this serine residue is changed to Phe (S3F). The *tm5848* deletion allele of *cil-7* removes the third and part of the fourth exon, producing an out-of -frame deletion (Figure 3F). *cil-7* deletion, myristoylation (G2D and S3F), and

deficiency/*my16* (data not shown) display similar phenotypes, indicating that each allele is likely a reduction or loss-of-function. We conclude that CIL-7 myristoylation is essential for its function in localizing PKD-2::GFP to cilia. Herein we further characterize the *tm5848* deletion allele.

We determined whether *cil-7* regulated localization of endogenous LOV-1. In wild-type males, an anti-LOV-1 monoclonal antibody detects endogenous LOV-1 at the cilia and the cell bodies of the CEM, HOB, and RnB neurons (Wang, Silva et al. 2014) (Figure 3G). In *cil*-7 males, LOV-1 accumulated at ciliary bases of CEM, HOB, and RnB neurons (Figure 3H). PKD-2::GFP and α-LOV-1 staining colocalized in both wild-type and *cil-7(tm5848)* males (Figure 5A-F). We conclude that CIL-7 is required for the localization of both PCs LOV-1 and PKD-2.

2.3.2 *cil-7* is Required for Release of Polycystin-Containing EVs

We previously reported that the EV-releasing ciliated neurons shed and release PC-containing EVs into the environment and that these EVs function in animal-animal communication (Wang, Silva et al. 2014). To determine if CIL-7 plays a role in EV shedding or release, we scored the number of GFP-tagged PKD-2 EVs released by the B type male tail neurons. We counted the number of PKD-2::GFP-containing EVs trapped by the cuticle of late L4 molting males. The majority of wild-type males exhibited an abundance of PKD-2::GFP EVs trapped in the molted cuticle (Figure 3I and J). In *cil*-7 males, fewer PKD-2::GFP EVs were released by male tail neurons (Figure 3I and 1J). We conclude that the

abnormal ciliary base accumulation of the polycystins in *cil-7* mutants may reflect a defect in EV shedding or release.

2.3.3 Myristoylation is Essential for CIL-7 Function

The EV-releasing RnB and HOB neurons are required by the male for response to hermaphrodite contact and location of the hermaphrodite's vulva. *cil-7(tm5848)* males were Rsp and Lov defective, similar to *lov-1*, *pkd-2*, and *klp-6* mutants (Figure 3K and L). A full length CIL-7::GFP translation fusion reporter rescued the mating defects of *cil-7(tm5848)* males, demonstrating that this reporter is functional (Figure 3K). By contrast, the myristoylated mutant, CIL-7(G2D)::GFP failed to rescue the mating defects of *cil-7(tm5848)* males (Figure 3K), which is consistent with myristoylation being essential for CIL-7 function.

C. elegans males will leave a food source in search of a mate if no hermaphrodite is present. If both food and a mate are present, males are retained in the food source (Barrios, Nurrish et al. 2008). Mate searching behavior is a form of sex drive and requires the RnB neurons and functional LOV-1 and PKD-2 (Barrios, Nurrish et al. 2008). To our surprise, neither the *klp-6* nor *cil-7* single mutant displays a defect in mate searching behavior: their probability of leaving (P_L) food in search of a mate was not significantly different from wild-type (Figure 3M). However, the *cil-7; klp-6* double mutant was defective in mate searching (Figure 3M). The *cil-7; pkd-2* and *pkd-2; klp-6* double mutants resembled the *pkd-2* single mutant, indicating that *pkd-2* is epistatic to *cil-7* and *klp-6*. Combined, these results suggest that, with respect to

male mate searching, *klp-6* and *cil-7* act in genetically redundant pathways that converge on *pkd-2*.

2.3.4 *cil-7* is Expressed in the 27 EV-Releasing Ciliated Sensory Neurons

A *cil-7* transcriptional GFP reporter (*cil-7* promoter (*Pcil-7::gfp*)) was expressed in the 27 EV-releasing neurons in males and in the six EV-releasing IL2 neurons in hermaphrodites (Figure 6A). The translational and functional CIL-7::GFP reporter localized to cell bodies (excluding nuclei), dendrites, axons, and the cilia and ciliary bases of the EV-releasing sensory neurons (Figure 6B). Interestingly, CIL-7::GFP was visible in EVs in 100% of males scored. While the myristoylation mutant CIL-7(G2D)::GFP did not perturb the overall distribution of CIL-7 within neurons (Figure 6C), CIL-7(G2D)::GFP was not enriched at ciliary bases and CIL-7(G2D)::GFP-containing EVs were observed in less than 50% of animals scored (Figure 6D-F). We conclude that CIL-7 is EV cargo, and that the CIL-7 myristoylation motif is required for efficient targeting or tethering of CIL-7 to EVs.

2.3.5 CIL-7 EVs are Released in a *klp-6* Dependent Manner

Similar to *cil-7*, the kinesin-3 KLP-6 is expressed in EV releasing neurons (Peden, Barr 2005), is required for response and vulva location behavior (Peden, Barr 2005) but not sex drive (Figure 3M), and regulates release of PC-containing EVs (Wang, Silva et al. 2014). To determine if *klp-6* controls CIL-7 EV release, we examined CIL-7::GFP in *klp-6* mutant animals. In *klp-6(my8)* mutants, CIL-7::GFP accumulated at ciliary bases of CEM and IL2 sensory neurons (Figure 7B), which is consistent with CIL-7 being EV cargo and *klp-6* mutants being

defective in EV release. In the *cil-7* mutant, KLP-6::GFP was not altered (Figure 7D). The latter result is not surprising given that, unlike CIL-7, KLP-6 functions within the cilium (Morsci, Barr 2011) and is not a cargo of ciliary EVs (Wang, Silva et al. 2014).

2.3.6 EVs Accumulate in the Cephalic Lumen of *cil-7* Males

We used Transmission Electron Microscopy (TEM) to analyze the ultrastructure of EV-releasing neurons in *cil-7(tm5848)* animals. In the wild-type male cephalic sensillum, EVs are found in the cephalic lumenal space that is created by the encapsulating cuticle, socket, and sheath cells, and that surrounds the CEM and CEP neurons (Wang, Silva et al. 2014). In hermaphrodites, EVs are not found in the cephalic lumen that lacks a CEM neuron (Wang, Silva et al. 2014). In *klp-6* mutant males, a large number of EVs accumulate in the cephalic lumen (Wang, Silva et al. 2014). In *cil-7* mutant males, an abundance of EVs were also observed in the lumen, spanning approximately the space between the level of the adherens junction connecting the sheath and socket cell, and to the level of the distal dendrite below the transition zone (Figure 8A'-3D'). This lumenal space was also distended and increased in volume compared to wild-type (Figure 8E and F). The *cil-7* lumenal space distension may be the result of increased quantity of EVs. Sheath cell spanning volumes of the CEM and CEP were not significantly different between wild-type and *cil-7* males, suggesting that EV shedding into the sheath cell lumen is not perturbed (Figure 8G and data not shown). In wild-type males, diameters of the EVs range from 46 nm-237 nm with a mean ± SD of 129.1 ± 49.4, consistent with published results (Wang, Silva et

al. 2014). *cil-7* animals have a similar EV diameter distribution with a mean ± SD of 131.8 ± 43.3. However, *cil-7* animals showed a slightly positive skew (skewness, wild-type: 0.46, *cil-7*: 0.57) suggesting that *cil-7* mutants possess a higher count of larger diameter vesicles (Figure 8H and I). CEM ciliary ultrastructure appeared normal in *cil-7* mutant males. We conclude that CIL-7 is both a cargo of EVs (Figure 6D and E) and a regulator of EV biogenesis.

2.3 Discussion

Here we identify the novel ciliary protein CIL-7 that is required for PC-mediated sensory signaling and regulates EV biogenesis, particularly, the release of PKD-2::GFP containing EVs into the environment. Myristoylation is essential for CIL-7 function, including its association with EVs (Figure 6D-F) and its role in PC-dependent mating behaviors (Figure 3K). N-myristoylation is used by proteins for membrane anchoring, including ciliary localization of proteins in *Trypanosome* flagella, *C. elegans* sensory neurons, mammalian photoreceptors, and retinal pigment epithelial cells (Ramulu, Nathans 2001, Wright, Baye et al. 2011, Evans, Schwarz et al. 2010, Maric, Epting et al. 2010). In Jurkat T-cells, myristoylation signals target proteins to EVs (Shen, Wu et al. 2011). In the *cpk* mouse model of PKD, the *cpk* mutation lies in the Cystin gene, which encodes a myristoylated cilia- and EV-associated protein (Hogan, Manganelli et al. 2009, Tao, Bu et al. 2009). The Cystin myristoylation signal is necessary for ciliary targeting in inner medullary collecting duct cells (Tao, Bu et al. 2009). Ours is the first identification of a cis-acting motif that is essential for EV targeting *in vivo* and

demonstrates that our *C. elegans* system has the power to identify EV biogenesis regulators, EV cargo, and EV targeting sequences.

Ultrastructural analysis indicates that *C. elegans* EVs may bud from the base of the cilium and, in living animals, GFP-tagged EVs are released from the cuticular pore to the environment (Figure 3J, Figure 6E) (Wang, Silva et al. 2014). How are EVs shed, transported from the lumen, and released to the environment? *klp-6* and *cil-7* may control EV biogenesis as positive regulators of EV release (Figure 9A) or negative regulators of shedding (Figure 9B). In *Chlamydomonas*, polystyrene microspheres adhere to and are moved bidirectionally along the flagellar surface (Bloodgood 1988, Bloodgood 1995). Intraflagellar transport (IFT) drives flagellar gliding motility and the transport of the major flagellar surface glycoprotein protein FMG1-B (Shih, Engel et al. 2013). When an anti-FMG1-B antibody is attached to beads, beads and IFT trains move in similar speeds. In Ctenophores, or comb jellies, individual cells are transported distally up the surface of the cilia, independent of ciliary beating, to build the statolith, a gravity-sensing organ (Noda, Tamm 2014). In a similar scenario, IFT and KLP-6 may propel EVs along the external ciliary surface (Figure 9A). In this model, EVs express unidentified surface proteins that may act between CIL-7 and a motor. EVs would move in a KLP-6-dependent and IFT-dependent manner, consistent with PKD-2::GFP EV release being blocked in *klp-6* and IFT mutant backgrounds (Wang, Silva et al. 2014). Alternatively, CIL-7 and KLP-6 may be negative regulators of EV shedding (Figure 9B). In either

scenario, the absence of *cil-7* or *klp-6* results in the accumulation of EVs in the cephalic lumen (Figure 9C,D).

In *Chlamydomonas*, *C. elegans*, and *mammals*, EVs are closely associated with cilia (Wood, Huang et al. 2013, Hogan, Manganelli et al. 2009, Wang, Silva et al. 2014, Pampliega, Orhon et al. 2013, Tanaka, Okada et al. 2005) suggesting that the cilium is essential in EV-mediated communication or that EVs are important for the health of the cilium. Alternatively, EVs may not be important for ciliary structure but rather the integrity or function of the sensory organ. Consistent with this possibility, *cil-7* and *klp-6* EV release mutants have normal CEM cilia, accumulate EVs in the distended lumen of the cephalic sensory organ (Figure 8), and are defective in the male mating behaviors (Figure 3K-M).

In addition to their role in intercellular signaling, EVs also signal between animals and between species. In *C. elegans* and Drosophila, EVs act as animal-to-animal communication devices (Wang, Silva et al. 2014, Corrigan, Redhai et al. 2014). EVs also function as interspecies signaling agents. The gastrointestinal gut nematode Heligmosomoides polygyrus secretes and transfers EVs containing miRNAs to modulate the innate immune response of mammalian cells (Buck, Coakley et al. 2014). Therefore, the release of EVs has broad implications in communication between cells, between organisms, and between species. While homologs are found in many invertebrate genomes, CIL-7 is absent from vertebrate genomes. In the past decade, evolutionary genetics has shown that genes come and go along lineages with amazing

fluidity, even genes that play essential physiological and developmental roles such as miRNAs or transcription factors. Another gene could do the job of CIL-7 in vertebrates; the primary sequence might be diverged but secondary structure conserved. Identifying EV release regulators such as CIL-7 will provide insight to mechanisms controlling EV biogenesis and signaling, and the relationship between cilia, EVs, and disease.

2.4 Materials and Methods

Strains and Maintenance

Transgenic reporters used: *myIs1 [PKD-2::GFP + Punc-122::GFP] IV*, *myEx686 [Pklp-6::GFP::gKLP-6_3'UTR + pBX]*, *myEx815 [Pcil-7::gCIL-7::GFP_3'UTR + ccRFP]*, *myEx816 [Pcil-7::GFP_3'UTR + ccRFP]*, *myEx847 [Pcil-7::gCIL-7G(2)->D::GFP_3'UTR + ccRFP]*

Alleles used:

LGI: *cil-7(my16)*, *cil-7(gk688330)*, *cil-7(tm5848)*

LGIII: *klp-6(my8)*

LGIV: *pkd-2(sy606)*

LGV: *him-5(e1490)*

Strain list:

CB169: *unc-31(e169) IV*

CB1490: *him-5(e1490) V*

PT9: *pkd-2(sy606) IV ; him-5(e1490) V*

PT495: *myIs1 IV ; him-5(e1490) V*

PT1194: *klp-6(my8) III ; him-5(e1490) V*

PT1197: *klp-6(my8) III ; pkd-2(sy606) IV ; him-5(e1490) V*

PT1646: *my16 ; myIs1 pkd-2(sy606) IV; him-5(e1490) V*

PT2681: *cil-7(tm5848) I ; myIs1 IV ; him-5(e1490) V*

PT2682: *cil-7(tm5848) I ; him-5(e1490) V*

PT2687: *him-5(e1490)V;myEx815[Pcil-7::gCIL-7::GFP_3'UTR+ccRFP]*

PT2688: *him-5(e1490) V ; myEx816[Pcil-7::GFP_3'UTR+ccRFP]*

PT2763: *cil-7(gk688330) I ; myIs1 IV ; him-5(e1490) V*

PT2764: *cil-7(tm5848)I;him-5(e1490)V; myEx815[Pcil-7::gCIL-7::GFP_3'UTR+ccRFP]*

PT2765: *him-5(e1490)V;myEx847[Pcil-7::gCIL-7G(2)->D::GFP_3'UTR+ccRFP]*

PT2766: *cil-7(tm5848)I; him-5(e1490)V;myEx847[Pcil-7::gCIL-7G(2)->D::GFP_3'UTR+ccRFP]*

PT2768: *cil-7(tm5848) I ; klp-6(my8) III ; him-5(e1490) V*

PT2770: *cil-7(tm5848) I ; pkd-2(sy606) IV ; him-5(e1490) V*

PT2773: *klp-6(my8) III; him-5(e1490) V; myEx815[Pcil-7::gCIL-7::GFP_3'UTR+ccRFP]*

PT2776: *cil-7(tm5848)I; him-5(e1490)V; myEx686[Pklp-6::GFP::gKLP-6_3'UTR+pBX]*

General Molecular Biology:

Mapping:

SNP mapping was performed following the protocol written in the Davis et al., 2005 paper (Davis, Hammarlund et al. 2005). Following SNP mapping deficiency mapping was done, and it was found that the following deficiencies complemented the *my16* Cil defect: hDf17, qDf7, qDf6, dxDf1, qDf3, tDf3. However, *my16* and sDf4 failed to complement. These results narrowed down the *my16* location region to -2.265 cM and +0.08 cM. Subsequently, after deficiency mapping Whole Genome Sequencing (WGS) courtesy of Dr. Richard Poole of Dr. Oliver Hobert's lab was undertaken and from within this above mentioned region W03G9.7 was shown to be relevant. W03G9.7 was further amplified as a single gene construct in order to determine if it could rescue the *my16* Cil phenotype. *gk688330* is a missense SNP and the nucleotide change involves the G5->A change. *tm5848* is an out-of-frame deletion covering part of the 3rd and 4th exons resulting in a frameshift.

Construct Generation:

The CIL-7 transcriptional and translational reporters were generated by PCR fusion (Hobert 2002). The promoter used was generated to be 564 base pairs long. This promoter was amplified by using standard PCR techniques and following known conditions when using Phusion DNA Polymerase. The promoter was generated as a genomic clone. The fluorescent GFP was amplified off of the pPD95.75 Plasmid from the Fire Lab. Both the CIL-7 transcriptional and

translational reporters were introduced into the *C. elegans* germline by microinjection. The transcriptional reporter was injected at a concentration of 35ng/µl and the translational reporter was injected at a concentration of 1ng/µl. Injecting the translational reporter at 10 ng/µl was found to cause neuron cell damage. The single gene fragment of CIL-7 that rescued the *cil-7(my16)* phenotype also included the CIL-7 promoter and was injected at 0.3 ng/ µl.

PCR fusion products were amplified from genomic DNA. Primers sets used for PCR fusion products are the following and are labeled as published (Hobert 2002):

CIL-7 transcriptional reporter (*myEx816*): Primer A (P1W03G9.7) 5'GCTGGGAGTCGATACATGGT3'; Primer B (P2W03G9.7tr) 5'TTCTTCTCCTTTACTCAGTGAAGAGCCCATAATCAGC3'; Primer C (P3W03G9.7tr) 5'GGGCTCTTCACTGAGTAAAGGAGAAGAACTTTTCACT3'; Primer D (P4GFP3'UTR) 5'CAAACCCAAACCTTCTTCCG3'

CIL-7 translational reporter (*myEx815*): Primer A (P1W03G9.7) 5'GCTGGGAGTCGATACATGGT 3'; Primer B (P2W03G9.7tl) 5'TTCTTCTCCTTTACTATGATGTGCAGACTTCTTCTTTC3'; Primer C (P3W03G9.7tl) 5'AGTCTGCACATCATAGTAAAGGAGAAGAACTTTTCACT3'; Primer D (P4GFP3'UTR) 5'CAAACCCAAACCTTCTTCCG3'

The W03G9.7 single gene rescue product was amplified off the WRM069cF09 fosmid using the following primer set: 5'CTCAACAGCAGCGACAACAT3'; 5'GCTGGGAGTCGATACATGGT3'

Imaging:

All imaging was performed using a Zeiss Axio Imager.D1m microscope using a 100X objective with a Q imaging Regtiga-SRV camera. Images were viewed using Metamorph Version 7.7.7.0 software (Molecular Devices). Images were taken at 5 MHz Gain and 200ms Exposure.

Images were processed using AutoQuant X, Auto Deblur Gold WF Version X2.2.2 software (Media Cybernetics) and subsequently with Adobe Photoshop CS3 Extended Version 10.0 software. Young adult male *C. elegans* were picked at the L4 stage and imaged 24 hours later.

C. elegans were imaged using 5% agarose pads and allowed to remain in 5ul 50mM for 3 minutes for anesthetization.

Transmission Electron Microscopy:

cil-7 and wild-type young adult animals were fixed using high-pressure freeze fixation and freeze substitution in 2% OsO_4 + 2% water in acetone as the primary fixative (Weimer 2006). Samples were slowly freeze substituted in an RMC freeze substitution device, before infiltration with Embed-812 plastic resin. For TEM, serial sections (75 nm thickness) of fixed animals were collected on copper slot grids coated with formvar and evaporated carbon and stained with 4% uranyl

acetate in 70% methanol, followed by washing and incubating with aqueous lead citrate. Images were captured on a Philips CM10 transmission electron microscope at 80kV with a Morada 11 megapixel TEM CCD camera driven by iTEM software (Olympus Soft Imaging Solutions).

Extracellular Vesicle Scoring:

Adult males can release LOV-1 and PKD-2 EVs from all the cilia of all B type sensory neurons, and EVs released from the RnB cilia can be trapped in a molted tail cuticle of late L4 males where the rays and fan are fully developed (Wang, Silva et al. 2014). Late L4 males were chosen for ease of scoring since the molted tail cuticle conveniently traps any EV released from the exposed cilium of the RnB neurons. Late L4 males were picked for imaging where the shedding cuticle surrounding the tail could be easily visualized. EVs were quantified by generating Z-stacks taken for at least 20 animals for each strain of interest. Imaged Z-stacks were quantified to have either 0 PKD-2::GFP tagged EV particles, 1-9 EV particles, or greater than 10 EV particles.

Cephalic Lumen Scoring:

Both wild-type and *cil-7* measurements were derived from serial section TEM images. Measurements of the inner sheath cell border and the CEM and CEP cell outline were taken in order to estimate the area of the sheath cell lumen. The measurements were taken with the top adherens junction made by the sheath cell with the socket cell as the starting point. The lower ending point for

taking measurements was the bottom adherens junction made by the sheath cell with the CEM-CEP distal dendrites. In order to obtain volumes, the areas measured were multiplied by the section thickness. In order to obtain the sheath cell lumen volume, the total lumen volume was subtracted by the corresponding sum of the CEM and CEP volumes. A total of four CEM sensilla were measured in each wild-type and *cil-7* animal.

EV Diameter Scoring:

The TEM images of a wild-type animal were scored for the diameter of EVs in the cephalic lumen of the dorsal right, dorsal left, and ventral left quadrants. The TEM images of a *cil-7* animal were scored for the diameter of EVs in the cephalic lumen of the dorsal right, ventral right, and ventral left quadrants. The longest possible diameter for each EV was selected for both the wild-type and *cil-7* animals. EVs scored were located approximately between the sheath and socket cell adherens junction connection and below the transition zone at the distal dendrite level. Images scored were with a Morada 11 megapixel TEM CCD camera driven by iTEM software (Olympus Soft Imaging Solutions). Images were analyzed using Metamorph Version 7.7.7.0 software (Molecular Devices) and ImageJ 1.49k (Wayne Rasband, National Institutes of Health, USA, http://imagej.nih.gov/ij).

Antibody Staining:

Animals were staged young adults and washed off plates with M9. Antibody staining against LOV-1 was performed using a Modified Finney Ruvkun protocol [(Bettinger, Lee et al. 1996);Wormatlas.org]. The monoclonal LOV-1 primary antibody was generated by Abmart (Wang, Silva et al. 2014). It was created against the extracellular domain, which encompasses the first 900 amino acids of LOV-1. The secondary antibody used was α mouse Alexa Fluor ® 568 donkey anti-mouse IgG (H + L) (2 mg/ml) by Invitrogen ™. The primary antibody was used at a concentration of 1:200 and the secondary antibody was used at a concentration of 1:2000.

Behavioral Assays:

Male Mating Assay: The mating behavioral assay including the response and location of vulva efficiency of males was performed as described (Bae, Kim et al. 2009, Barr, Sternberg 1999).

Male Leaving Assay: Male leaving behavior was measured as described (Barrios, Ghosh et al. 2012).

Bioinformatics and Computer Tools:

Domain analysis: The myristoylation motif was identified using the NMT – The MYR Predictor [http://mendel.imp.ac.at/myristate/SUPLpredictor.htm]. The leucine zipper was identified using the ExPASy PROSITE

[http://prosite.expasy.org/]. The coiled-coil domains were identified using the COILS server [http://www.ch.embnet.org/software/COILS_form.html].

Phylogenetic Analysis:

W03G9.7 protein sequence was used as a query for NCBI p-BLAST, cutoff 1e-5. A multiple sequence alignment was created using full length sequences from hits identified using Muscle through MEGA6. MEGA6 was used to create a maximum likelihood phylogenetic tree from the sequences sites with a site coverage cut off of 7% and using the JTT substitution model. 100 bootstrap replications were used. The gene sequence for W03G9.7 was retrieved from Ensembl and was used as an NBCI nBLAST query, using 1e-5 as a cutoff.

Statistical Analysis:

Software used was GraphPad Prism 5 Version 5.03 (GraphPad Software) and Microsoft Excel Version 14.0.7128.5000 (Microsoft Corporation).

2.5 Figures for Chapter 2

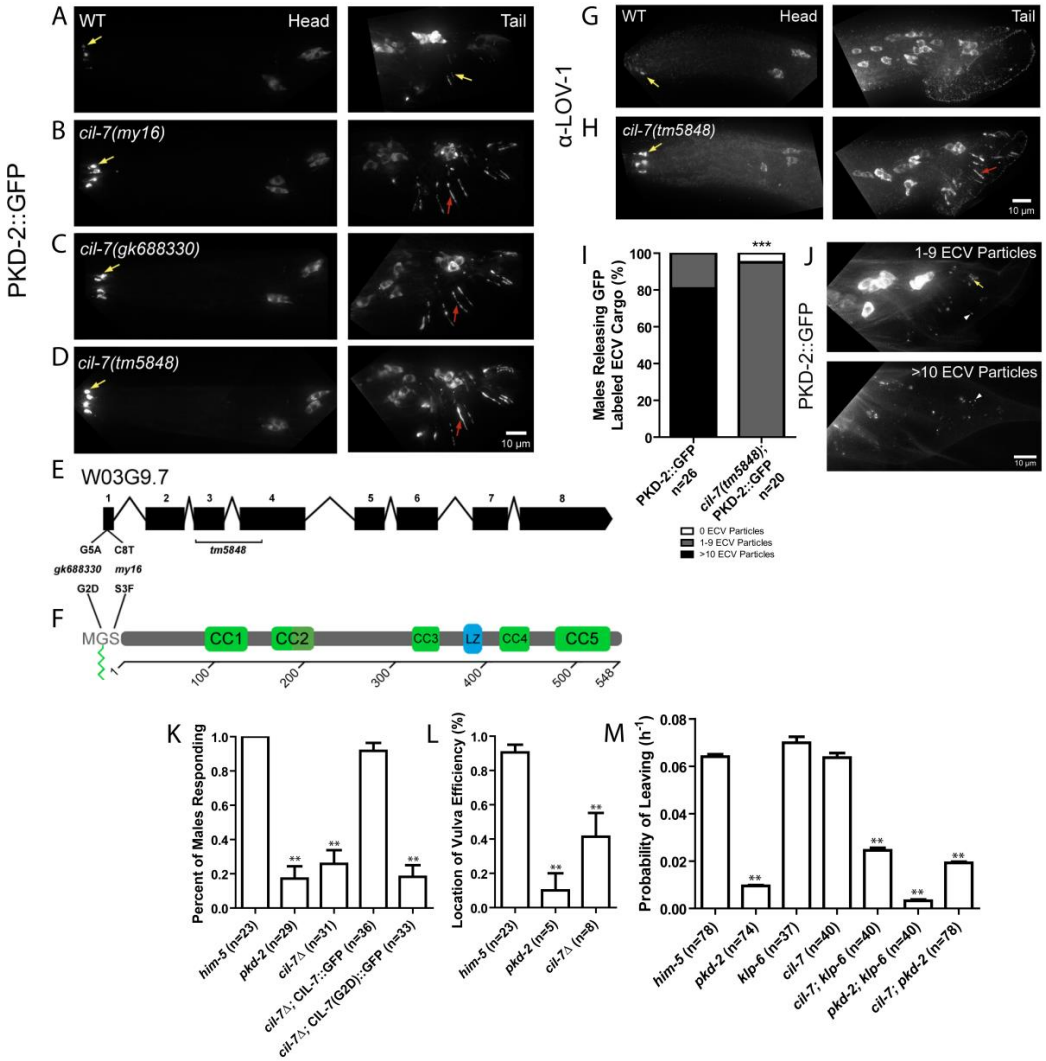

Figure 3. *cil-7* is Required for the Localization of the Polycystins and Male Mating Behaviors

(A) PKD-2::GFP localized to the cilia and cell bodies of the CEM, RnB, and HOB neurons of males. (B-D) In *cil-7(my16)*, *cil-7(gk688330)* and *cil-7(tm5848)* males, head CEM neurons and tail HOB and RnB neurons accumulated PKD-2::GFP along the dendrites and cilia. (E) *cil-7* genomic structure. *my16* (C8->T) and *gk688330* (G5->A) are missense SNPs. *tm5848* is an out-of-frame deletion. (F) *cil-7* encodes a predicted protein with an N-terminal myristoylation motif, five coiled-coil domains, and a leucine zipper. (G) The α-LOV-1 antibody showed that endogenous LOV-1 localized to the cilia and cell bodies of the CEM, HOB, and RnB neurons. (H) In *cil-7(tm5848)* males, endogenous LOV-1 accumulated at the base and along the cilia of the CEM neurons. Excess LOV-1 appeared along the cilia and the dendrites of the RnB neurons. (I) In the cuticle of L4 molting wild-type males, greater than 10 PKD-2::GFP containing EV particles are observed in 80% of animals scored. In *cil-7(tm5848)* L4 molting males, much fewer PKD-2::GFP containing EVs were observed. (J) Representative images of PKD-2::GFP EV particle ranges (1-9 or >10) that were observed to be trapped in the molted tail cuticle of late L4 males. (K) *cil-7(tm5848)* males did not respond to hermaphrodite contact. The translational reporter P*cil-7*::CIL-7::GFP rescued the response defect of *cil-7(tm5848)* males. By contrast, the myristoylation defective reporter P*cil-7*::CIL-7(G2D)::GFP failed to rescue response defects of *cil-7(tm5848)* males. (L) *cil-7(tm5848)* males were location of vulva (Lov) defective. (M) *cil-7(tm5848)* males were not leaving assay defective (nonLas).

The *cil-7(tm5848); klp-6(sy511)* double mutant was Las, unlike the *cil-7(tm5848)* or *klp-6(sy511)* single mutants. In panel I ***p < 0.0001 by the Mann-Whitney test. In panel K, data was analyzed with Fisher's exact test between all groups, followed by Holm-Bonferroni multiple comparison adjustment with a total alpha of 0.01 (**). In panel L data was analyzed with the pairwise Mann-Whitney U-test between all groups, followed by Holm-Bonferroni multiple comparison adjustment with a total alpha of 0.01 (**). In panel M probability of leaving (P_L) values were compared by Holm-Bonferroni multiple comparison adjustment with a total alpha of 0.01 (**). Yellow arrow – cilia; red arrow – dendrite; white arrowhead – EV particle.

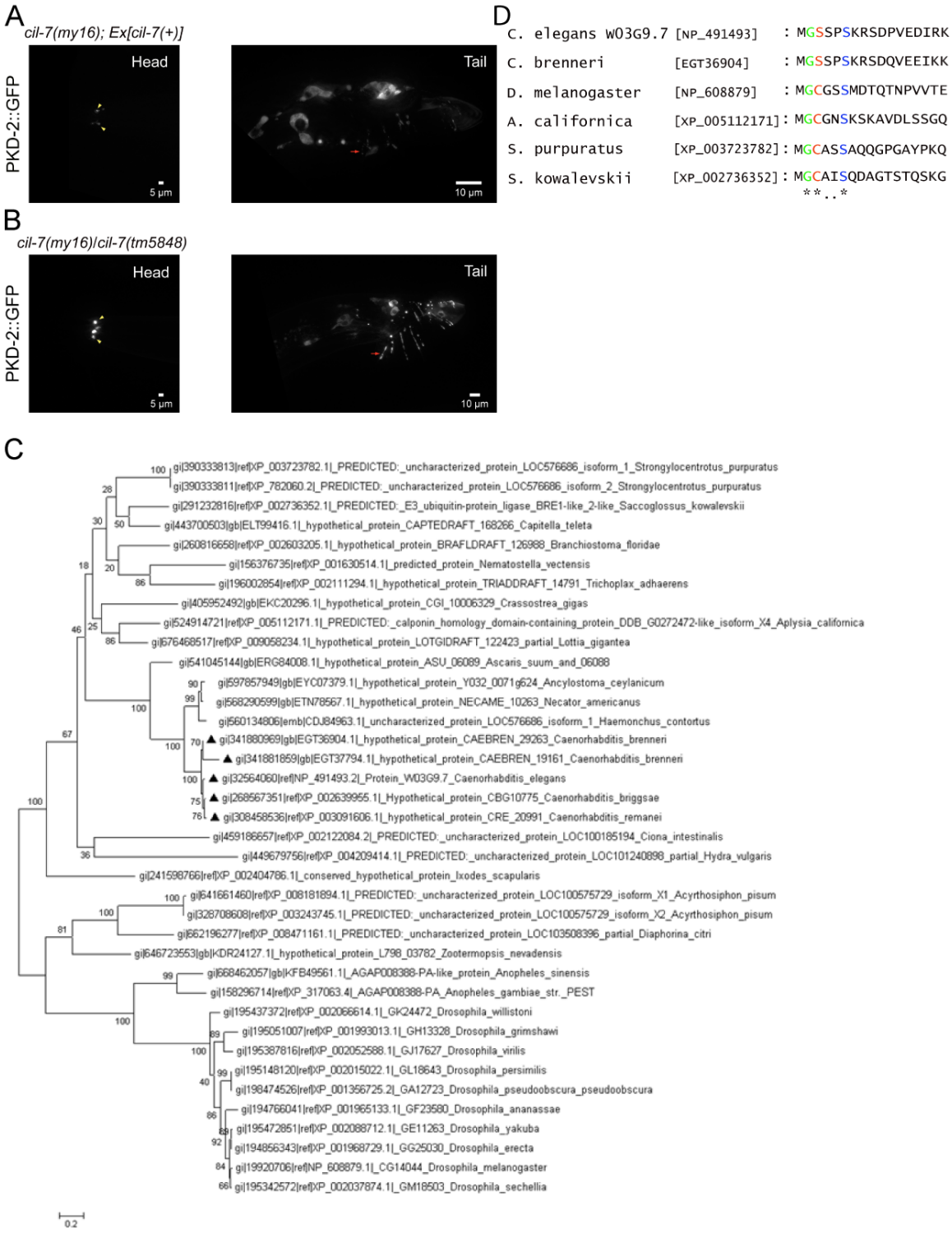
A
cil-7(my16); Ex[cil-7(+)]
PKD-2::GFP
Head
Tail
5 µm
10 µm
B
cil-7(my16)/cil-7(tm5848)
PKD-2::GFP
Head
Tail
5 µm
10 µm
D
C. elegans W03G9.7 [NP_491493] : MGSSPSKRSDPVEDIRK
C. brenneri [EGT36904] : MGSSPSKRSDQVEEIKK
D. melanogaster [NP_608879] : MGCGSSMDTQTNPVVTE
A. californica [XP_005112171] : MGCGNSKSKAVDLSSGQ
S. purpuratus [XP_003723782] : MGCASSAQQGPGAYPKQ
S. kowalevskii [XP_002736352] : MGCAISQDAGTSTQSKG
C
gi|390333813|ref|XP_003723782.1|_PREDICTED:_uncharacterized_protein_LOC576686_isoform_1_Strongylocentrotus_purpuratus
gi|390333811|ref|XP_782060.2|_PREDICTED:_uncharacterized_protein_LOC576686_isoform_2_Strongylocentrotus_purpuratus
gi|291232816|ref|XP_002736352.1|_PREDICTED:_E3_ubiquitin-protein_ligase_BRE1-like_2-like_Saccoglossus_kowalevskii
gi|443700503|gb|ELT99416.1|_hypothetical_protein_CAPTEDRAFT_168266_Capitella_teleta
gi|260816658|ref|XP_002603205.1|_hypothetical_protein_BRAFLDRAFT_126988_Branchiostoma_floridae
gi|156376735|ref|XP_001630514.1|_predicted_protein_Nematostella_vectensis
gi|196002854|ref|XP_002111294.1|_hypothetical_protein_TRIADDRAFT_14791_Trichoplax_adhaerens
gi|405952492|gb|EKC20296.1|_hypothetical_protein_CGI_10006329_Crassostrea_gigas
gi|524914721|ref|XP_005112171.1|_PREDICTED:_calponin_homology_domain-containing_protein_DDB_G0272472-like_isoform_X4_Aplysia_californica
gi|676468517|ref|XP_009058234.1|_hypothetical_protein_LOTGIDRAFT_122423_partial_Lottia_gigantea
gi|541045144|gb|ERG84008.1|_hypothetical_protein_ASU_06089_Ascaris_suum_and_06088
gi|597857949|gb|EYC07379.1|_hypothetical_protein_Y032_0071g624_Ancylostoma_ceylanicum
gi|568290599|gb|ETN78567.1|_hypothetical_protein_NECAME_10263_Necator_americanus
gi|560134806|emb|CDJ84963.1|_uncharacterized_protein_LOC576686_isoform_1_Haemonchus_contortus
gi|341880969|gb|EGT36904.1|_hypothetical_protein_CAEBREN_29263_Caenorhabditis_brenneri
gi|341881859|gb|EGT37794.1|_hypothetical_protein_CAEBREN_19161_Caenorhabditis_brenneri
gi|32564060|ref|NP_491493.2|_Protein_W03G9.7_Caenorhabditis_elegans
gi|268567351|ref|XP_002639955.1|_Hypothetical_protein_CBG10775_Caenorhabditis_briggsae
gi|308458536|ref|XP_003091606.1|_hypothetical_protein_CRE_20991_Caenorhabditis_remanei
gi|459186657|ref|XP_002122084.2|_PREDICTED:_uncharacterized_protein_LOC100185194_Ciona_intestinalis
gi|449679756|ref|XP_004209414.1|_PREDICTED:_uncharacterized_protein_LOC101240898_partial_Hydra_vulgaris
gi|241598766|ref|XP_002404786.1|_conserved_hypothetical_protein_Ixodes_scapularis
gi|641661460|ref|XP_008181894.1|_PREDICTED:_uncharacterized_protein_LOC100575729_isoform_X1_Acyrthosiphon_pisum
gi|328708608|ref|XP_003243745.1|_PREDICTED:_uncharacterized_protein_LOC100575729_isoform_X2_Acyrthosiphon_pisum
gi|662196277|ref|XP_008471161.1|_PREDICTED:_uncharacterized_protein_LOC103508396_partial_Diaphorina_citri
gi|646723553|gb|KDR24127.1|_hypothetical_protein_L798_03782_Zootermopsis_nevadensis
gi|668462057|gb|KFB49561.1|_AGAP008388-PA-like_protein_Anopheles_sinensis
gi|158296714|ref|XP_317063.4|_AGAP008388-PA_Anopheles_gambiae_str._PEST
gi|195437372|ref|XP_002066614.1|_GK24472_Drosophila_willistoni
gi|195051007|ref|XP_001993013.1|_GH13328_Drosophila_grimshawi
gi|195387816|ref|XP_002052588.1|_GJ17627_Drosophila_virilis
gi|195148120|ref|XP_002015022.1|_GL18643_Drosophila_persimilis
gi|198474526|ref|XP_001356725.2|_GA12723_Drosophila_pseudoobscura_pseudoobscura
gi|194766041|ref|XP_001965133.1|_GF23580_Drosophila_ananassae
gi|195472851|ref|XP_002088712.1|_GE11263_Drosophila_yakuba
gi|194856343|ref|XP_001968729.1|_GG25030_Drosophila_erecta
gi|19920706|ref|NP_608879.1|_CG14044_Drosophila_melanogaster
gi|195342572|ref|XP_002037874.1|_GM18503_Drosophila_sechellia
0.2

Figure 4. CIL-7 has Invertebrate Homologs that All Share a Predicted Myristoylation Motif

(A) The Cil phenotype of *cil-7(my16)* males could be rescued by injection (0.3 ng/µl) of a *cil-7* genomic clone. (B) The *tm5848* allele failed to complement the *my16* allele producing Cil males. (C) Maximum likelihood phylogenetic tree of protein sequences showing similarity to W03G9.7 (pBLAST <1e-5). Sequences showing the conserved myristoylation sequence (1-17aa) are marked with a triangle. (D) Conservation of the N-terminal glycine is exhibited in invertebrate homologs.

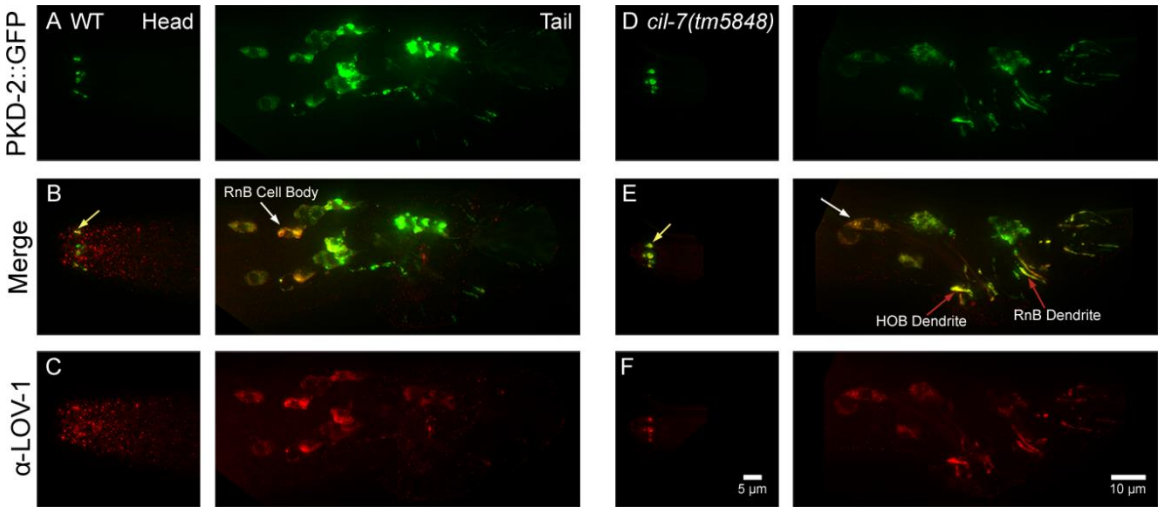
PKD-2::GFP
Merge
α-LOV-1
A WT
Head
Tail
D cil-7(tm5848)
B
RnB Cell Body
E
HOB Dendrite
RnB Dendrite
C
F
5 µm
10 µm

Figure 5. LOV-1 and PKD-2 Accumulated Abnormally in the Male-Specific Neurons of *cil-7(tm5848)* Males

(A-C) PKD-2::GFP and α-LOV-1 colocalized in CEM, RnB, and HOB neurons.

(D-F) PKD-2::GFP and α-LOV-1 abnormally accumulated at the ciliary bases of CEM, RnB, and HOB neurons. Yellow arrow – cilia; red arrow – dendrite; white arrow – cell body.

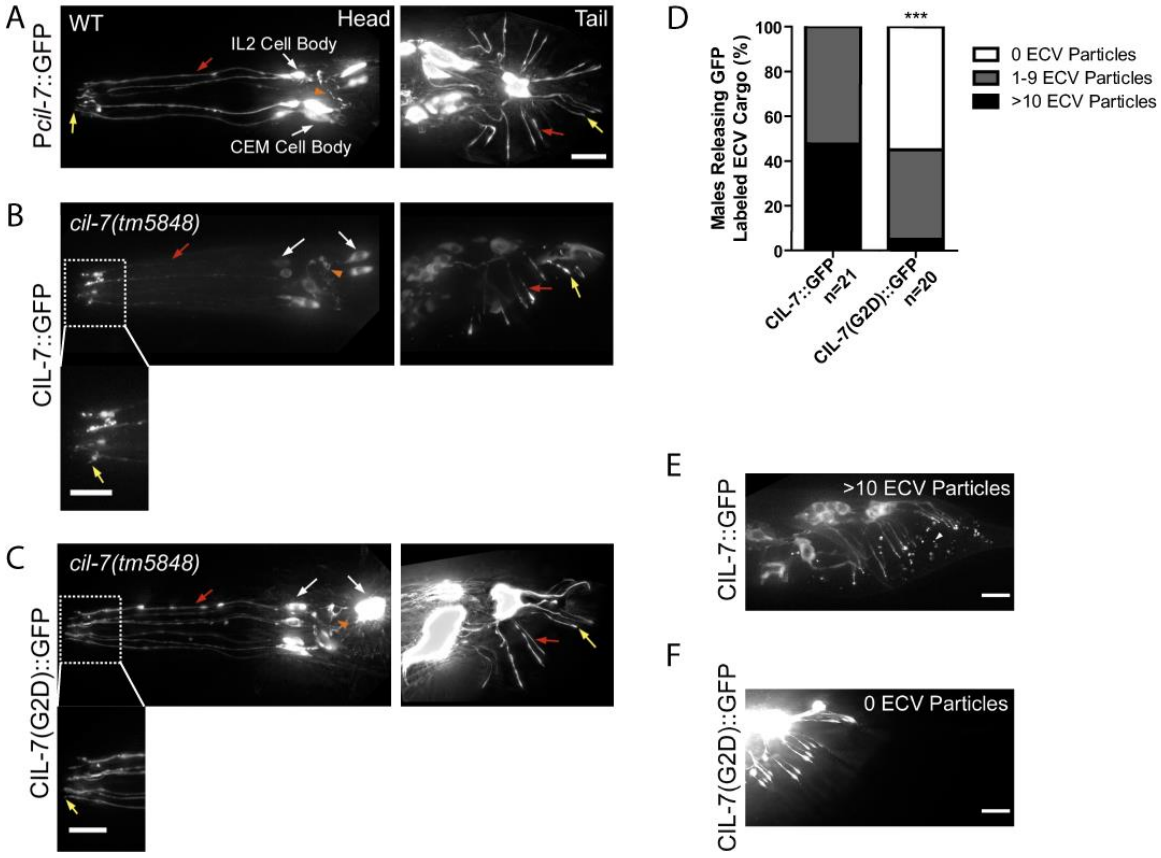
A
WT
Head
Tail
IL2 Cell Body
CEM Cell Body
Pcil-7::GFP
B
cil-7(tm5848)
CIL-7::GFP
C
cil-7(tm5848)
CIL-7(G2D)::GFP
D
***
Males Releasing GFP Labeled ECV Cargo (%)
100
80
60
40
20
0
0 ECV Particles
1-9 ECV Particles
>10 ECV Particles
CIL-7::GFP n=21
CIL-7(G2D)::GFP n=20
E
CIL-7::GFP
>10 ECV Particles
F
CIL-7(G2D)::GFP
0 ECV Particles

Figure 6. *cil-7* is Expressed in the 27 EV-Releasing Neurons and is Targeted to EVs in a Myristoylation-Motif Dependent Manner

(A) P*cil-7*::GFP was expressed in CEM, RnB, HOB, and IL2 neurons. (B) P*cil-7*::CIL-7::GFP in *cil-7(tm5848)* males localized throughout neurons, including cilia, but was excluded from the nucleus. P*cil-7*::CIL-7::GFP rescues *cil-7(tm5848)* defects (Figure 3K), indicating that this reporter is functional. (C) P*cil-7*::CIL-7(G2D)::GFP in *cil-7(tm5848)* males localized throughout neurons, including cilia, but was excluded from the nucleus. P*cil-7*::CIL-7(G2D)::GFP does not rescue *cil-7(tm5848)* defects (Figure 3K), indicating that this reporter is not functional. (D) CIL-7::GFP as EV cargo was trapped in the molted tail cuticle of the late L4 male in a range from either 1-9 EV particles or >10 EV particles per male tail. The CIL-7(G2D)::GFP myristoylation mutant is not efficiently targeted to EVs. (E) In 100% of animals, CIL-7::GFP was observed in the molted tail cuticle in varying ranges and here depicted is an example of >10 EV particles. (F) In less than 50% of animals, CIL-7 (G2D)::GFP was observed as EV cargo. In panel E ***$p < 0.0001$ by the Mann-Whitney test. Yellow arrow – cilia; red arrow – dendrite; white arrow – cell body; orange arrowhead – axon; white arrowhead – EV particle.

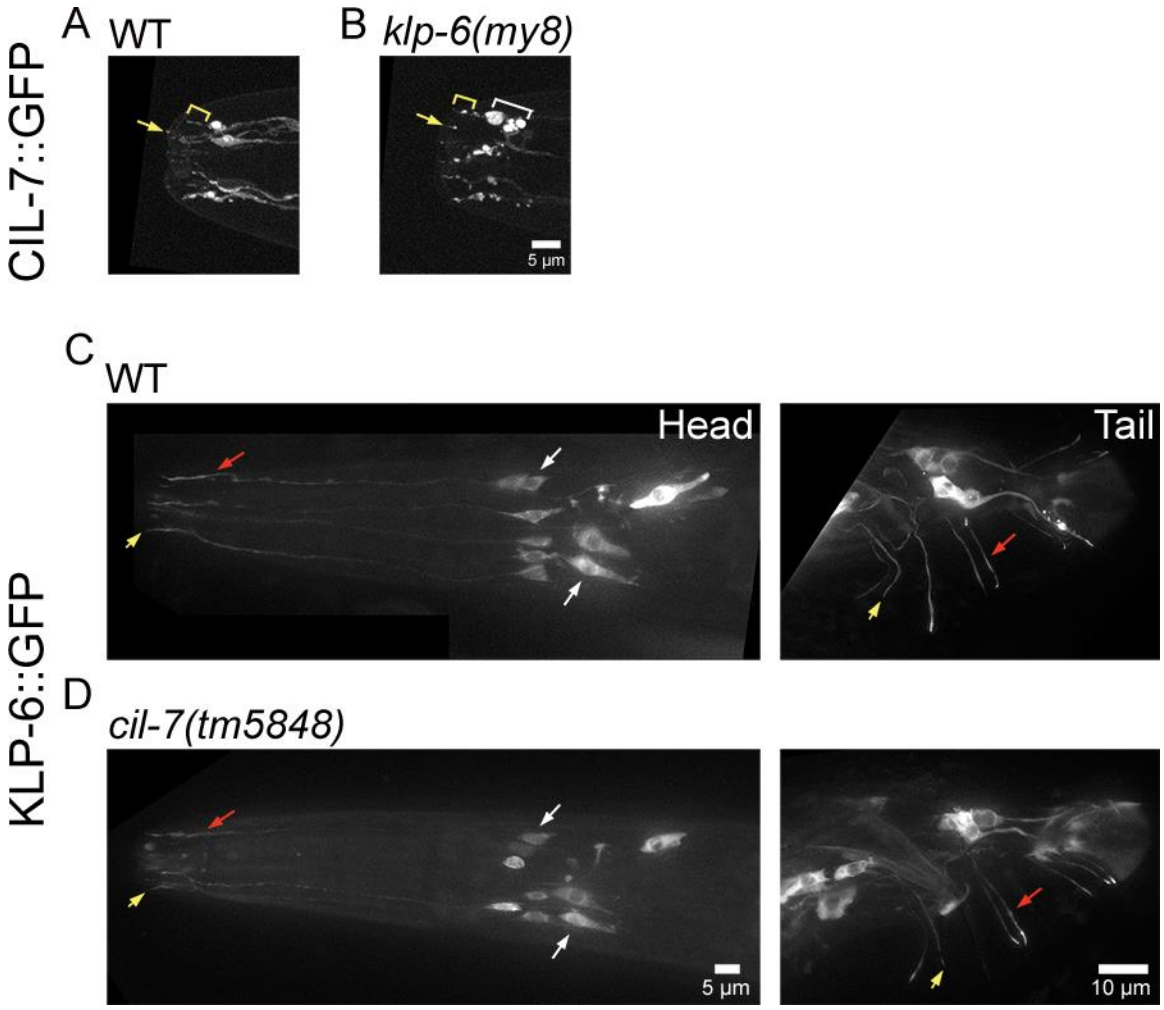
A WT
B klp-6(my8)
CIL-7::GFP
5 µm
C WT
Head
Tail
KLP-6::GFP
D cil-7(tm5848)
5 µm
10 µm

Figure 7. The Kinesin-3 KLP-6 is Required for Normal CIL-7 Localization

(A) In wild-type CEM and IL2 neurons P*cil-7*::CIL-7::GFP localized to cilia and along dendrites. (B) In *klp-6(my8)*, CIL-7::GFP abnormally localized to bases of cilia as nodules. (C,D) In wild-type, KLP-6::GFP was found throughout the male sensory neurons and the shared IL2 neurons. In a *cil-7(tm5848)* mutant, the localization of KLP-6::GFP was not altered. Yellow arrow and yellow bracket – cilia; white bracket – cilia base; red arrow – dendrite; white arrow – cell body.

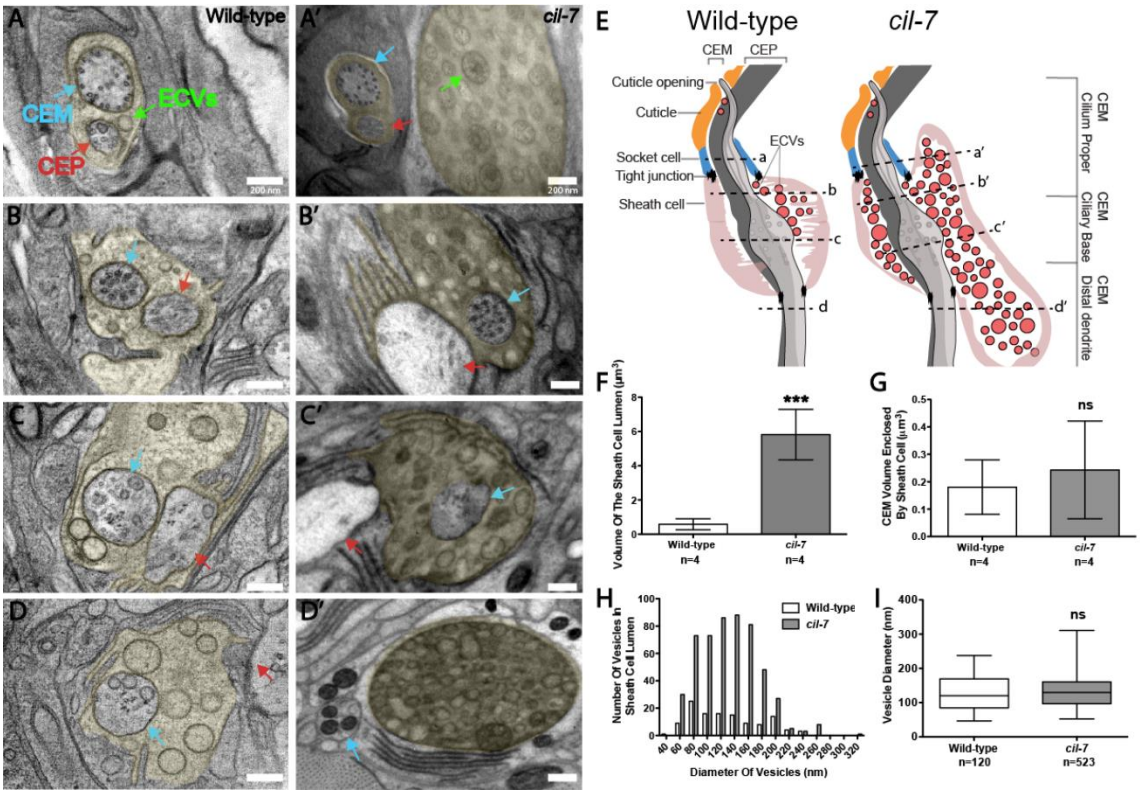
A
Wild-type
CEM
ECVs
CEP
200 nm
A′
cil-7
200 nm
B
B′
C
C′
D
D′
E
Wild-type
cil-7
CEM
CEP
Cuticle opening
Cuticle
Socket cell
Tight junction
Sheath cell
ECVs
a
b
c
d
a′
b′
c′
d′
CEM Cilium Proper
CEM Ciliary Base
CEM Distal dendrite
F
Volume Of The Sheath Cell Lumen (μm³)
***
Wild-type n=4
cil-7 n=4
G
CEM Volume Enclosed By Sheath Cell (μm³)
ns
Wild-type n=4
cil-7 n=4
H
Number Of Vesicles In Sheath Cell Lumen
Wild-type
cil-7
Diameter Of Vesicles (nm)
I
Vesicle Diameter (nm)
ns
Wild-type n=120
cil-7 n=523

Figure 8. *cil-7* Mutants Accumulate EVs in the Cephalic Lumen, but are not Defective in Ciliogenesis

(A-D) Series of TEM images in a wild-type animal displaying EVs in the sheath cell lumen that surrounds the CEM and CEP distal dendritic region (Lumen is pseudo-colored yellow). (A'-D') TEM images revealed that *cil-7(tm5848)* males had excessive amounts of EVs in the sheath cell lumen. Both CEM and CEP axonemes appeared normal. (E) Cartoon depiction of the *cil-7(tm5848)* mutant phenotype compared to wild-type, including increased quantity of EVs and distended sheath cell lumen. Dashed lines indicate the location of the A-D and A'-D' TEM images with respect to the cephalic sensillum. (F) Compared to wild-type (0.6 ± 0.3), the *cil-7(tm5848)* sheath cell lumen is ten times larger (5.8 ± 1.5) (average volume ± SD, µm; n = number of cephalic sensilla). (G) The average CEM volume enclosed within the sheath cell that surrounds the CEM distal dendrite and axoneme in wild-type was 0.2 ± 0.1 and the corresponding volume in *cil-7(tm5848)* was 0.24 ± 0.2 (average volume ± SD, µm; n = number of cephalic sensilla), indicating that the integrity of CEM neurons is normal in *cil-7* mutants. (H) Compared to wild-type, *cil-7(tm5848)* animals displayed an increased number of EVs in the sheath cell lumen. The frequency distribution of EV sizes in *cil-7(tm5848)* was slightly favored toward EVs above the average mean (skewness of the diameter distribution as measured in Microsoft Excel, wild-type =0.46, *cil-7*=0.57). (I) The average EV diameter of wild-type and *cil-7(tm5848)* males was not significantly different. The average EV diameter for wild-type was 129.1 ± 49.4 and the average vesicle diameter for *cil-7(tm5848)* was 131.8 ± 43.3 (average diameter ± SD, nm). In panel F ***$p < 0.001$ by the

Unpaired t-Test. In panel G a non-significant difference was determined by the Unpaired t-Test. In panel I a non-significant difference was determined by the Welch's t-Test. Panel I includes Box-and-Whisker plots where the plot is divided into limits that are each 25% of the population.

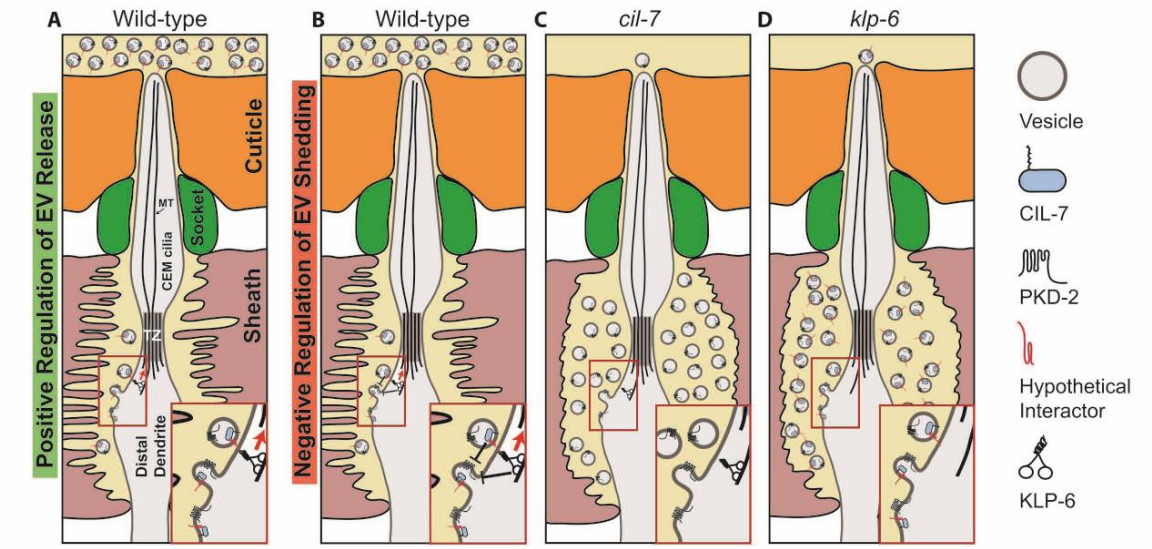
A
Wild-type
B
Wild-type
C
cil-7
D
klp-6
Positive Regulation of EV Release
Negative Regulation of EV Shedding
Cuticle
Socket
Sheath
MT
CEM cilia
TZ
Distal Dendrite
Vesicle
CIL-7
PKD-2
Hypothetical Interactor
KLP-6

Figure 9. Models for CIL-7 and KLP-6 Mediated EV Biogenesis

(A) KLP-6 and CIL-7 may be positive regulators of EV environmental release. In this model, EVs bud from the ciliary base and are shed into the cephalic lumen. From here, KLP-6 and intraflagellar transport (IFT) may propel EVs along the ciliary membrane surface to the cuticular opening. Myristoylated, membrane-associated CIL-7 is EV cargo that acts with an unidentified transmembrane tether. The tethered EV binds a ciliary surface protein that is transported by KLP-6 and IFT. Inset shows the EV tethered to an unidentified protein such as a flagellar membrane glycoprotein. (B) CIL-7 and KLP-6 may act as dual negative regulators of EV shedding. Inset depicts a negative feedback loop with CIL-7 and KLP-6 acting in concert to regulate EV shedding. (C, D) In the absence of *cil-7* or *klp-6* as a positive regulator of EV release or negative regulator of EV shedding, the net result is an accumulation of EVs within the cephalic lumen. In both models, *klp-6* acts within the EV-releasing ciliated sensory neurons, whereas *cil-7* may act in the EV-releasing cell or in the EV itself.

2.6 References

BAE, Y.K., KIM, E., L'HERNAULT, S.W. and BARR, M.M., 2009. The CIL-1 PI 5-phosphatase localizes TRP Polycystins to cilia and activates sperm in C. elegans. *Current biology : CB,* **19**(19), pp. 1599-1607.

BAE, Y.K., LYMAN-GINGERICH, J., BARR, M.M. and KNOBEL, K.M., 2008. Identification of genes involved in the ciliary trafficking of C. elegans PKD-2. *Developmental dynamics : an official publication of the American Association of Anatomists,* **237**(8), pp. 2021-2029.

BARR, M.M., DEMODENA, J., BRAUN, D., NGUYEN, C.Q., HALL, D.H. and STERNBERG, P.W., 2001. The Caenorhabditis elegans autosomal dominant polycystic kidney disease gene homologs lov-1 and pkd-2 act in the same pathway. *Current biology : CB,* **11**(17), pp. 1341-1346.

BARR, M.M. and STERNBERG, P.W., 1999. A polycystic kidney-disease gene homologue required for male mating behaviour in C. elegans. *Nature,* **401**(6751), pp. 386-389.

BARRIOS, A., GHOSH, R., FANG, C., EMMONS, S.W. and BARR, M.M., 2012. PDF-1 neuropeptide signaling modulates a neural circuit for mate-searching behavior in C. elegans. *Nature neuroscience,* **15**(12), pp. 1675-1682.

BARRIOS, A., NURRISH, S. and EMMONS, S.W., 2008. Sensory regulation of C. elegans male mate-searching behavior. *Current biology : CB,* **18**(23), pp. 1865-1871.

BETTINGER, J.C., LEE, K. and ROUGVIE, A.E., 1996. Stage-specific accumulation of the terminal differentiation factor LIN-29 during Caenorhabditis elegans development. *Development (Cambridge, England),* **122**(8), pp. 2517-2527.

BLOODGOOD, R.A., 1995. Flagellar surface motility: gliding and microsphere movements. *Methods in cell biology,* **47**, pp. 273-279.

BLOODGOOD, R.A., 1988. Gliding motility and the dynamics of flagellar membrane glycoproteins in Chlamydomonas reinhardtii. *The Journal of protozoology,* **35**(4), pp. 552-558.

BUCK, A.H., COAKLEY, G., SIMBARI, F., MCSORLEY, H.J., QUINTANA, J.F., LE BIHAN, T., KUMAR, S., ABREU-GOODGER, C., LEAR, M., HARCUS, Y., CERONI, A., BABAYAN, S.A., BLAXTER, M., IVENS, A. and MAIZELS, R.M., 2014. Exosomes secreted by nematode parasites transfer small RNAs to

mammalian cells and modulate innate immunity. *Nature communications,* **5**, pp. 5488.

CAI, Y., FEDELES, S.V., DONG, K., ANYATONWU, G., ONOE, T., MITOBE, M., GAO, J.D., OKUHARA, D., TIAN, X., GALLAGHER, A.R., TANG, Z., XIE, X., LALIOTI, M.D., LEE, A.H., EHRLICH, B.E. and SOMLO, S., 2014. Altered trafficking and stability of polycystins underlie polycystic kidney disease. *The Journal of clinical investigation,* **124**(12), pp. 5129-5144.

CEVIK, S., SANDERS, A.A., VAN WIJK, E., BOLDT, K., CLARKE, L., VAN REEUWIJK, J., HORI, Y., HORN, N., HETTERSCHIJT, L., WDOWICZ, A., MULLINS, A., KIDA, K., KAPLAN, O.I., VAN BEERSUM, S.E., MAN WU, K., LETTEBOER, S.J., MANS, D.A., KATADA, T., KONTANI, K., UEFFING, M., ROEPMAN, R., KREMER, H. and BLACQUE, O.E., 2013. Active transport and diffusion barriers restrict Joubert Syndrome-associated ARL13B/ARL-13 to an Inv-like ciliary membrane subdomain. *PLoS genetics,* **9**(12), pp. e1003977.

CHACON-HESZELE, M.F., CHOI, S.Y., ZUO, X., BAEK, J.I., WARD, C. and LIPSCHUTZ, J.H., 2014. The exocyst and regulatory GTPases in urinary exosomes. *Physiological reports,* **2**(8), pp. 10.14814/phy2.12116. Print 2014 Aug 1.

CORRIGAN, L., REDHAI, S., LEIBLICH, A., FAN, S.J., PERERA, S.M., PATEL, R., GANDY, C., WAINWRIGHT, S.M., MORRIS, J.F., HAMDY, F., GOBERDHAN, D.C. and WILSON, C., 2014. BMP-regulated exosomes from Drosophila male reproductive glands reprogram female behavior. *The Journal of cell biology,* **206**(5), pp. 671-688.

DAVIS, M.W., HAMMARLUND, M., HARRACH, T., HULLETT, P., OLSEN, S. and JORGENSEN, E.M., 2005. Rapid single nucleotide polymorphism mapping in C. elegans. *BMC genomics,* **6**, pp. 118.

EISENHABER, F., EISENHABER, B., KUBINA, W., MAURER-STROH, S., NEUBERGER, G., SCHNEIDER, G. and WILDPANER, M., 2003. Prediction of lipid posttranslational modifications and localization signals from protein sequences: big-Pi, NMT and PTS1. *Nucleic acids research,* **31**(13), pp. 3631-3634.

EVANS, R.J., SCHWARZ, N., NAGEL-WOLFRUM, K., WOLFRUM, U., HARDCASTLE, A.J. and CHEETHAM, M.E., 2010. The retinitis pigmentosa protein RP2 links pericentriolar vesicle transport between the Golgi and the primary cilium. *Human molecular genetics,* **19**(7), pp. 1358-1367.

GODSEL, L.M. and ENGMAN, D.M., 1999. Flagellar protein localization mediated by a calcium-myristoyl/palmitoyl switch mechanism. *The EMBO journal,* **18**(8), pp. 2057-2065.

GYORGY, B., SZABO, T.G., PASZTOI, M., PAL, Z., MISJAK, P., ARADI, B., LASZLO, V., PALLINGER, E., PAP, E., KITTEL, A., NAGY, G., FALUS, A. and BUZAS, E.I., 2011. Membrane vesicles, current state-of-the-art: emerging role of extracellular vesicles. *Cellular and molecular life sciences : CMLS,* **68**(16), pp. 2667-2688.

HOBERT, O., 2002. PCR fusion-based approach to create reporter gene constructs for expression analysis in transgenic C. elegans. *BioTechniques,* **32**(4), pp. 728-730.

HOGAN, M.C., MANGANELLI, L., WOOLLARD, J.R., MASYUK, A.I., MASYUK, T.V., TAMMACHOTE, R., HUANG, B.Q., LEONTOVICH, A.A., BEITO, T.G., MADDEN, B.J., CHARLESWORTH, M.C., TORRES, V.E., LARUSSO, N.F., HARRIS, P.C. and WARD, C.J., 2009. Characterization of PKD protein-positive exosome-like vesicles. *Journal of the American Society of Nephrology : JASN,* **20**(2), pp. 278-288.

MARIC, D., EPTING, C.L. and ENGMAN, D.M., 2010. Composition and sensory function of the trypanosome flagellar membrane. *Current opinion in microbiology,* **13**(4), pp. 466-472.

MARIC, D., MCGWIRE, B.S., BUCHANAN, K.T., OLSON, C.L., EMMER, B.T., EPTING, C.L. and ENGMAN, D.M., 2011. Molecular determinants of ciliary membrane localization of Trypanosoma cruzi flagellar calcium-binding protein. *The Journal of biological chemistry,* **286**(38), pp. 33109-33117.

MAURER-STROH, S., EISENHABER, B. and EISENHABER, F., 2002. N-terminal N-myristoylation of proteins: prediction of substrate proteins from amino acid sequence. *Journal of Molecular Biology,* **317**(4), pp. 541-557.

MORSCI, N.S. and BARR, M.M., 2011. Kinesin-3 KLP-6 regulates intraflagellar transport in male-specific cilia of Caenorhabditis elegans. *Current biology : CB,* **21**(14), pp. 1239-1244.

NODA, N. and TAMM, S.L., 2014. Lithocytes are transported along the ciliary surface to build the statolith of ctenophores. *Current biology : CB,* **24**(19), pp. R951-2.

O'HAGAN, R., WANG, J. and BARR, M.M., 2014. Mating behavior, male sensory cilia, and polycystins in Caenorhabditis elegans. *Seminars in cell & developmental biology,* **33**, pp. 25-33.

PAMPLIEGA, O., ORHON, I., PATEL, B., SRIDHAR, S., DIAZ-CARRETERO, A., BEAU, I., CODOGNO, P., SATIR, B.H., SATIR, P. and CUERVO, A.M., 2013. Functional interaction between autophagy and ciliogenesis. *Nature,* **502**(7470), pp. 194-200.

PEDEN, E.M. and BARR, M.M., 2005. The KLP-6 kinesin is required for male mating behaviors and polycystin localization in Caenorhabditis elegans. *Current biology : CB,* **15**(5), pp. 394-404.

RAMULU, P. and NATHANS, J., 2001. Cellular and subcellular localization, N-terminal acylation, and calcium binding of Caenorhabditis elegans protein phosphatase with EF-hands. *The Journal of biological chemistry,* **276**(27), pp. 25127-25135.

RESH, M.D., 2013. Covalent lipid modifications of proteins. *Current biology : CB,* **23**(10), pp. R431-5.

SHEN, B., WU, N., YANG, J.M. and GOULD, S.J., 2011. Protein targeting to exosomes/microvesicles by plasma membrane anchors. *The Journal of biological chemistry,* **286**(16), pp. 14383-14395.

SHIH, S.M., ENGEL, B.D., KOCABAS, F., BILYARD, T., GENNERICH, A., MARSHALL, W.F. and YILDIZ, A., 2013. Intraflagellar transport drives flagellar surface motility. *eLife,* **2**, pp. e00744.

TANAKA, Y., OKADA, Y. and HIROKAWA, N., 2005. FGF-induced vesicular release of Sonic hedgehog and retinoic acid in leftward nodal flow is critical for left-right determination. *Nature,* **435**(7039), pp. 172-177.

TAO, B., BU, S., YANG, Z., SIROKY, B., KAPPES, J.C., KISPERT, A. and GUAY-WOODFORD, L.M., 2009. Cystin localizes to primary cilia via membrane microdomains and a targeting motif. *Journal of the American Society of Nephrology : JASN,* **20**(12), pp. 2570-2580.

TULL, D., NADERER, T., SPURCK, T., MERTENS, H.D., HENG, J., MCFADDEN, G.I., GOOLEY, P.R. and MCCONVILLE, M.J., 2010. Membrane protein SMP-1 is required for normal flagellum function in Leishmania. *Journal of cell science,* **123**(Pt 4), pp. 544-554.

UTSUMI, T., SATO, M., NAKANO, K., TAKEMURA, D., IWATA, H. and ISHISAKA, R., 2001. Amino acid residue penultimate to the amino-terminal gly residue strongly affects two cotranslational protein modifications, N-myristoylation and N-acetylation. *The Journal of biological chemistry,* **276**(13), pp. 10505-10513.

WANG, J., SILVA, M., HAAS, L.A., MORSCI, N.S., NGUYEN, K.C., HALL, D.H. and BARR, M.M., 2014. C. elegans Ciliated Sensory Neurons Release Extracellular Vesicles that Function in Animal Communication. *Current biology : CB,* **24**(5), pp. 519-525.

WEIMER, R.M., 2006. Preservation of C. elegans tissue via high-pressure freezing and freeze-substitution for ultrastructural analysis and immunocytochemistry. *Methods in molecular biology (Clifton, N.J.),* **351**, pp. 203-221.

WOOD, C.R., HUANG, K., DIENER, D.R. and ROSENBAUM, J.L., 2013. The cilium secretes bioactive ectosomes. *Current biology : CB,* **23**(10), pp. 906-911.

WRIGHT, K.J., BAYE, L.M., OLIVIER-MASON, A., MUKHOPADHYAY, S., SANG, L., KWONG, M., WANG, W., PRETORIUS, P.R., SHEFFIELD, V.C., SENGUPTA, P., SLUSARSKI, D.C. and JACKSON, P.K., 2011. An ARL3-UNC119-RP2 GTPase cycle targets myristoylated NPHP3 to the primary cilium. *Genes & development,* **25**(22), pp. 2347-2360.

Chapter 3: Conclusion

3.1 Key Findings

3.1.1 Myristoylated CIL-7 is Essential for Loading of EV Cargo and Regulating EV Abundance

The myristoylated protein CIL-7 is expressed in all EV-releasing neurons and is EV cargo. The myristoylation moiety is necessary for CIL-7 function and may direct CIL-7 to particular membrane domains, including EV membrane prior to budding. This population of myristoylated CIL-7 acts to regulate the amount of PKD-2 at the cilia base; unmyristoylated CIL-7 cannot properly traffic PKD-2, leading to ciliary accumulation. Thus, protein myristoylation can play a role in targeting proteins to ciliary EVs. Not all cilia proteins are destined to be EV cargo as CIL-7 is; OSM-6, CHE-11, OSM-3, KAP-1, KLP-6, TBB-4, ODR-10, and soluble GFP are not EV cargo, indicating selectivity (Wang, Silva et al. 2014).

TEM imaging shows that in *cil-7* mutants there is an abundance of EVs in the cephalic lumen. This accumulation may be due to EV over-production or failure in the re-uptake of EVs (which may be mediated by EV-cilia membrane fusion). It is a future challenge to tease out which possibility may be occurring.

3.2 Limitations

3.2.1 Fluorescent Reporter Overexpression May Cause Cilia Defects

One limitation is the overexpression of GFP-tagged reporters may not reflect endogenous protein localization or function. The utilization of such techniques as CRISPR, provides an advantage in the insertion of fluorescent tags (Frokjaer-

Jensen 2013). When injected at 10 ng/ µl, the CIL-7::GFP reporter had deleterious effects on neuronal integrity. However, the CIL-7::GFP reporter injected at 1 ng/ µl was functional and rescued the mating response defect of *cil-7(tm5848)* animals. Moreover, the reporter did not cause dominant effects in mating behavior.

3.2.2 Correlation between Tail EV Quantification and Cephalic EV Accumulation

In this work, I measured GFP-tagged EVs released from the L4 male tail cilia and assumed a correlation with the presence of EVs in the cephalic lumen. In the future, developing a method to measure release from CEM ciliated neurons is important. Additionally, resolving the mechanism by which CIL-7 traffics EVs is essential and challenging. If the role of CIL-7 were regulating the quantity of EVs shed into the cephalic lumen, then we would need to determine strategies to visualize EV budding and shedding.

3.2.3 CIL-7 Encodes Few Domains of Predicted Function

Structure-function analysis by mutating key domains may help discriminate between a role in EV active transport or in negatively regulating EV shedding. However, a limitation is that CIL-7 does not have any major known domains that could help in deciphering its function.

3.2.4 Difficulty of Scoring CIL-7 Localization in Cilia Mutants

Analyzing the localization of CIL-7::GFP in a *klp-11*, *osm-3*, and *klp-6* mutant was difficult. To eliminate observer bias, scoring was performed with the

experimenter blinded. I also showed images of a particular phenotype to a colleague in order to get an outside opinion to combat biasing myself. My methods relied heavily on qualitative and not quantitative descriptions of a phenotype. For example, CIL-7::GFP but not CIL-7^{S3F}::GFP levels are reduced in an *unc-119* mutant. The next step would be to measure quantitatively *cil-7* mRNA or CIL-7 protein levels.

3.2.5 Difficulties in Kymograph Acquisition

In studying neuronal transport, the main limitation in general is the acquiring of kymographs for velocity and other measurements. The acquiring of kymographs and deciphering of velocity lines can be subjective at times. That is why one must be consistent in defining a moving particle.

Also, acquisition of CIL-7::GFP kymographs proved challenging because CIL-7::GFP did not move in discrete puncta like PKD-2 or the IFT machinery. CIL-7::GFP appeared to move through the dendrites of CEM and RnB neurons. However, I was never able to acquire an adequate number of kymographs to obtain velocity measurements for CIL-7::GFP. Trying to capture the movement of CIL-7::GFP along cilia presented a similar challenge.

3.3 Future Directions

3.3.1 Cilia and EV membrane composition in *cil-1* mutants

PI(4,5)P_2 and PI(3,4,5)P_3 may also be involved in the localization of PKD-2::GFP. AGE-1 and DAF-18 regulate PKD-2::GFP localization and regulate the formation of these two phosphoinositide species. Thus the genetically encoded markers

for $PI(4,5)P_2$ and $PI(3,4,5)P_3$ should be examined in the *age-1* and *daf-18* mutants. An opposing enzyme to CIL-1 could be a PI(3)P 5-kinase, thus mutations or RNAi feeding against known PI(3)P 5-kinases could be combined with the *cil-1* mutant to see if the PKD-2::GFP accumulation phenotype is rescued.

Using the *cil-1* mutant and RNAi feeding against PIKI-1, AGE-1, and VPS-34 at the same time may be useful to see what happens to PKD-2::GFP localization as these enzymes may act redundantly.

3.3.2 Effect of *cil-7* EVs on Male Behavior

It also could be determined whether an EV preparation from *cil-7* mutant animals could elicit a male backing/turning response. The limited amount of EVs released from a *cil-7* animal may not be bioactive and fail to elicit a backing/turning response.

3.3.3 Physical Interactors of CIL-7

Doing a pull down assay or western blot and then probing it for interactors would also give insight into whether or not CIL-7 was binding to other EV associated proteins. ExoCarta and Vesiclepedia (ExoCarta is used to access high quality exosomal datasets) compile lipid, RNA, and protein identified in different types of extracellular vesicles (Kalra, Simpson et al. 2012). *C. elegans* genes found in both the Barr Lab RNAseq data set and Vesiclepedia may be useful in determining epistasis with *cil-7* in vesicle shedding and release.

3.3.4 Physical and Genetic Interactions Between CIL-7/*cil-7* and UNC-119/*unc-119*

Vertebrate UNC119 (using yeast two-hybrid and *in vitro* pull down assays) can bind acylated G protein α-subunits, Arl2 and Arl3 (small Arf-like GTPases), src-type tyrosine kinases, and dynamin (Constantine, Zhang et al. 2012). In this collection of proteins that UNC-119 interacts with there are proteins in which the acyl side chain (myristoyl group) can bind the UNC119 β-sandwich cavity (Constantine, Zhang et al. 2012). Alleles of *C. elegans unc-119*, which alter the binding pocket could be tested in order to see their effect on CIL-7::GFP localization. CIL-7::GFP localization in an *unc-119* mutant where the myristoyl binding cavity is disrupted may create a CIL-7 localization pattern similar to non-myristoylatable CIL-7.

Pull down assays or western blots may be used to determine if CIL-7 binds directly to UNC-119. A positive interaction would lend credence to the observation where the CIL-7::GFP reporter looks reduced in the *unc-119* mutant.

3.3.5 Is CIL-7 Actually Myristoylated?

Myristoylation can be detected using radioactive [^{3}H]-myristic acid (Martin, Beauchamp et al. 2011). However, this is not the best technique; long exposure times are required for the incorporation of [^{3}H]-myristic acid (Martin, Vilas et al. 2008). One biochemical technique that can be used involves the incorporation of azido-myristate (a bio-orthogonal analog of myristate, 12 carbon with an ω -azido group) into proteins. The azido moiety is ligated to triarylphosphines that have FLAG or biotin that can be detected with Western blotting (Martin,

Beauchamp et al. 2011). A chemical ligation technique that involves click chemistry [Cu (I)-catalyzed (3 + 2) Huisgen cycloaddition reaction] can detect co-translational myristoylation as well as post-translational myristoylation. Cells can take up the ω-alkynl-myristate analog and incorporate it into proteins (Martin, Beauchamp et al. 2011). With click chemistry, the alkynl moiety can be linked with a probe like biotin in order to do affinity purification or Western blot (Martin, Beauchamp et al. 2011). For click chemistry to be utilized *cil-7* would need to be expressed in a cell culture line.

The CIL-7::GFP reporter was integrated to purify the protein and to perform mass spectrometry in order to see that CIL-7 is modified by the addition of myristoylation. The myristoylation mutant CIL-7(G2D)::GFP reporter could be integrated as well for performing mass spectrometry. Purification would require the production of antibodies against CIL-7 and non-myristoylated CIL-7. Mass spectrometry would allow the specific determination of a co-translational modification and the residue modified, but is more expensive, would require collaboration, and technique optimization. *cil-7* is only expressed in six cells in the hermaphrodite and 27 in the adult male, which may present a problem with protein detection.

3.4 References

BAE, Y.K., KIM, E., L'HERNAULT, S.W. and BARR, M.M., 2009. The CIL-1 PI 5-phosphatase localizes TRP Polycystins to cilia and activates sperm in C. elegans. *Current biology : CB,* **19**(19), pp. 1599-1607.

BALLA, T., 2013. Phosphoinositides: tiny lipids with giant impact on cell regulation. *Physiological Reviews,* **93**(3), pp. 1019-1137.

CONSTANTINE, R., ZHANG, H., GERSTNER, C.D., FREDERICK, J.M. and BAEHR, W., 2012. Uncoordinated (UNC)119: coordinating the trafficking of myristoylated proteins. *Vision research,* **75**, pp. 26-32.

FROKJAER-JENSEN, C., 2013. Exciting prospects for precise engineering of Caenorhabditis elegans genomes with CRISPR/Cas9. *Genetics,* **195**(3), pp. 635-642.

KALRA, H., SIMPSON, R.J., JI, H., AIKAWA, E., ALTEVOGT, P., ASKENASE, P., BOND, V.C., BORRAS, F.E., BREAKEFIELD, X., BUDNIK, V., BUZAS, E., CAMUSSI, G., CLAYTON, A., COCUCCI, E., FALCON-PEREZ, J.M., GABRIELSSON, S., GHO, Y.S., GUPTA, D., HARSHA, H.C., HENDRIX, A., HILL, A.F., INAL, J.M., JENSTER, G., KRAMER-ALBERS, E.M., LIM, S.K., LLORENTE, A., LOTVALL, J., MARCILLA, A., MINCHEVA-NILSSON, L., NAZARENKO, I., NIEUWLAND, R., NOLTE-'T HOEN, E.N., PANDEY, A., PATEL, T., PIPER, M.G., PLUCHINO, S., PRASAD, T.S., RAJENDRAN, L., RAPOSO, G., RECORD, M., REID, G.E., SANCHEZ-MADRID, F., SCHIFFELERS, R.M., SILJANDER, P., STENSBALLE, A., STOORVOGEL, W., TAYLOR, D., THERY, C., VALADI, H., VAN BALKOM, B.W., VAZQUEZ, J., VIDAL, M., WAUBEN, M.H., YANEZ-MO, M., ZOELLER, M. and MATHIVANAN, S., 2012. Vesiclepedia: a compendium for extracellular vesicles with continuous community annotation. *PLoS biology,* **10**(12), pp. e1001450.

MARTIN, D.D., BEAUCHAMP, E. and BERTHIAUME, L.G., 2011. Post-translational myristoylation: Fat matters in cellular life and death. *Biochimie,* **93**(1), pp. 18-31.

MARTIN, D.D., VILAS, G.L., PRESCHER, J.A., RAJAIAH, G., FALCK, J.R., BERTOZZI, C.R. and BERTHIAUME, L.G., 2008. Rapid detection, discovery, and identification of post-translationally myristoylated proteins during apoptosis using a bio-orthogonal azidomyristate analog. *FASEB journal : official publication of the Federation of American Societies for Experimental Biology,* **22**(3), pp. 797-806.

WANG, J., SCHWARTZ, H.T. and BARR, M.M., 2010. Functional specialization of sensory cilia by an RFX transcription factor isoform. *Genetics,* **186**(4), pp. 1295-1307.

WANG, J., SILVA, M., HAAS, L.A., MORSCI, N.S., NGUYEN, K.C., HALL, D.H. and BARR, M.M., 2014. C. elegans Ciliated Sensory Neurons Release Extracellular Vesicles that Function in Animal Communication. *Current biology : CB,* **24**(5), pp. 519-525.